NOVA SCHOOL OF SCIENCE & TECHNOLOGY

Chemistry Department

Ricardo Miguel Santos Viegas Velez

BSc in Chemical and Biochemical Engineering

Development of a nebulization platform for the pulmonary delivery of RNA lipid nanoparticles

Master in Chemical and Biochemical Engineering

NOVA University Lisbon

October, 2022

NOVA SCHOOL OF SCIENCE & TECHNOLOGY

Chemical Department

Development of a nebulization platform for the pulmonary delivery of RNA lipid nanoparticles

Ricardo Miguel Santos Viegas Velez

BSc in Chemical and Biochemical Engineering

Adviser: Doctor Luís Marques,
Scientist, Hovione

Co-advisers: Doctor Ana Aguiar Ricardo
Full Professor, NOVA University Lisbon

Doctor Susana Ramalhete
Analytical Scientist, Hovione

Examination Committee:

Chair: Doctor Mário Fernando José Eusébio
Full Professor, NOVA University Lisbon

Rapporteurs: Doctor Maria Luísa Teixeira de Azevedo Rodrigues Corvo
Full Professor, University Lisbon

Adviser: Doctor Luís Marques,
Scientist, Hovione

Members: Doctor Ana Aguiar Ricardo
Full Professor, NOVA University Lisbon

Master in Chemical and Biochemical Engineering
NOVA University Lisbon
October, 2022

Development of a nebulization platform for the pulmonary delivery of RNA lipid nanoparticles

ACKNOWLEDGMENTS

This thesis is the culmination of 5 years of hard work, effort, and dedication, and for that reason, I will start by thanking all the people who during these 5 years made it possible to reach this moment, from my friends from Coruche to my friends from university to my teachers, to my colleagues from the internship at INFARMED and to my futsal friends, all were important in this journey.

This journey could not have been done without the financial and emotional support of my family, especially my parents, Sandra and Fernando, and my grandparents, Maria and Mário. I know you made a lot of sacrifices to get me here and I hope you are proud of my journey.

During my 5 years of university and my thesis, I have to highlight the importance of João Nuno, Guilherme Gomes, Diogo Anselmo, Diogo Lobato, Diogo Bento, and Tiago Romanini. It was this group that supported me every day until this moment, from the university parties to the endless nights of study in building 7, they were always there to help me and to criticize me when necessary.

I also highlight Mariana Valadas, Leonor Laires, and Paulo Farinha, a group of colleagues working on a university project that after so much time spent together became a second family. Together we spent moments of high stress, moments of sadness, moments of immense happiness, and above all, many memories for which I can only thank you for everything.

In these 6 months of thesis work, I must firstly thank Hovione for the opportunity provided, as well as all its workers, masters, and doctoral students who helped me achieve the proposed objectives.

I would like to also thank Professor Ana Aguiar Ricardo for her support as a supervisor of my thesis as well as for the teachings that she transmitted to me during my academic career.

At Hovione I have to give a very special thanks to my supervisors, Susana Ramalhete and Luís Marques, for all the useful advices given for the elaboration of the thesis and my professional future, they were tireless from the first to the last day. I hope you are proud of the work we have achieved together.

Finally, I have to thank the doctoral student Patrícia Nunes for the advices given throughout the thesis and a special thanks to the doctoral students Rute Mota and Susana Farinha for all the help given over these months, they were the ones who accompanied me and taught me everything about the laboratory work that I performed and without them I would not achieve all the objectives proposed.

“The best way to have a good idea is to have a lot of ideas.”
Linus Pauling

Abstract

RNA can be used for the treatment of respiratory diseases. Yet, delivery of RNA to the lungs via inhalation without its degradation is still a challenge. The present work studied the delivery of RNA encapsulated into lipid nanoparticles (LNPs) via inhalation using a vibrating mesh nebulizer.

Two nucleic acids were encapsulated in LNPs and used as proof of concept: tRNA and mRNA. Production of LNPs composed of DOTAP, DSPC, Cholesterol, DMG-PEG 2000, and DC-Chol was performed through microfluidics.

tRNA LNPs' production was optimized to obtain a reproducible process. 19 batches were manufactured showing low variability between them regarding the key quality attributes particle size < 200 nm, PDI < 0.300, and encapsulation efficiency > 80 %. The stability post-production was evaluated under different storage conditions, being reported stable storage at 2-8 ºC up to 100 days.

To understand RNA LNPs stability and aerodynamic performance upon nebulization, a formulation screening was performed, comprising NaCl, PBS, Poloxamer 188, Tween 80, sucrose, and/or arginine. The formulation PBS with E %Tween 80 (W/V) containing tRNA encapsulated in LNPs presented the most favorable colloidal stability before and after nebulization. The good aerodynamic performance of the formulation proved its capacity to effectively deliver tRNA into the deep lungs.

The previous formulation was additionally tested for mRNA molecule. Its integrity was not compromised upon nebulization nor LNPs colloidal stability. The formulation complied with the referred quality attributes and showed an aerodynamic performance capable of delivering inhalable droplets of mRNA. Despite that, as the initial formulation was based on optimized tRNA LNPs (smaller RNA molecule), it should be further improved for mRNA.

This study pioneered a proof of concept for the delivery of mRNA and tRNA via inhalation through nebulized LNPs using a vibrating mesh nebulizer.

Microfluidics, Transfer RNA, Messenger RNA, Lipid nanoparticles, Nebulization, Aerodynamic performance.

RESUMO

O RNA é uma molécula que pode ser usada no tratamento de doenças respiratórias, mas a capacidade de atingir os pulmões por inalação sem haver degradação é um desafio. O presente trabalho estudou a capacidade de RNA encapsulado em nanopartículas lipídicas (LNPs) ser inalado usando um nebulizador de malha vibratória (VMN).

Neste trabalho, utilizaram-se e encapsularam-se dois tipos de RNA: tRNA e mRNA. Produziram-se LNPs compostas por DOTAP, DSPC, Colesterol, DMG-PEG 2000 e DC-Chol através de microfluídica.

A produção de tRNA LNPs foi otimizada para obter um processo reprodutível. Produziram-se 19 com baixa variabilidade dos critérios de qualidade: tamanho de partícula < 200 nm, PDI < 0,300 e eficiência de encapsulação > 80 %. A estabilidade pós-produção foi avaliada para diferentes condições de armazenamento, onde se obteve estabilidade das LNPs até 100 dias a 2-8 ºC.

Para compreender a estabilidade e o desempenho aerodinâmico após a nebulização, foram realizados testes com formulações com diferentes excipientes: NaCl, PBS, Poloxamer 188, Tween 80, sacarose e arginina. A formulação PBS com E % de Tween 80 (W/V) apresentou a estabilidade coloidal mais favorável antes e depois de nebulizada. O desempenho aerodinâmico desta formulação provou a sua capacidade para veicular tRNA nos pulmões com eficiência.

A formulação anterior foi testada com mRNA onde ficou demonstrado que a sua integridade e a sua estabilidade coloidal não foram comprometidas após a nebulização. A formulação apresentou um desempenho aerodinâmico capaz de fornecer gotículas inaláveis contendo mRNA nos pulmões com eficiência. Apesar disso, como a formulação foi baseada em LNPs de tRNA (RNA de menor tamanho), o procedimento deverá ser otimizado para a molécula de mRNA

Este estudo foi pioneiro na entrega de mRNA e tRNA através de nebulização usando um VMN.

Microfluidica, RNA Transferência, RNA Mensageiro, Nanopartículas Lipídicas, Nebulização, Performance Aerodinâmica.

CONTENTS

1 INTRODUCTION 1

1.1 Respiratory diseases and economic burden 1

1.2 RNA based therapies 2

1.2.1 RNA-based therapies history 2

1.2.2 RNA therapeutics 3

1.3 Challenges of RNA delivery 5

1.3.1 Delivery barriers 5

1.3.2 RNA delivery strategies in inhalation 6

1.3.3 Lipid nanoparticle composition 7

1.3.4 Importance of excipients 9

1.4 Lipid nanoparticles production 10

1.4.1 LNPs production methods 10

1.4.2 Ethanol injection method, and operational process parameters 11

1.5 Inhalation methods 13

1.5.1 Pressurized Metered-Dose inhaler (pMDI) Dry Powder Inhaler (DPI) 13

1.5.2 Nebulization: different types and comparison with previous methods 14

1.6 Quality attributes for inhaled RNA-LNPs 17

1.6.1 Particle Size 17

1.6.2 Surface Charge 18

1.6.3 Osmolarity 19

1.6.4 pH 19

1.6.5 Encapsulation Efficiency for RNA 20

1.6.6 RNA integrity: gel electrophoresis and HPLC 20

1.6.7 Aerodynamic particle size distribution 21

1.6.8 Delivered Dose of RNA 23

2 MATERIALS AND METHODS 25

2.1 Materials 25

2.2 Methods 26

2.2.1 LNPs production by Microfluidics 26

2.2.2 LNPs dialysis 28

2.2.3 Osmolarity 29

2.2.4 LNPs nebulization 29

2.2.5 Particle size and zeta potential 30

2.2.6 Encapsulation Efficiency 30

2.2.7 Aerodynamic particle size distribution 31

2.2.8 Delivered dose 32

2.2.9 RNA integrity 33

2.2.10 LNPs stability test 34

3 RESULTS AND DISCUSSION 35

3.1 tRNA LNPs production: troubleshooting, characterization, and stability 35

3.2 tRNA LNPs screening formulations for nebulization 39

3.3 Osmolarity's importance in LNPs nebulization 44

3.4 Nebulization of tRNA LNPs diluted formulations 45

3.5 Aerodynamic performance of nebulized formulations 47

3.6 Characterization of nebulized tRNA-LNPs in PBS E % T80 (1:10) formulation 50

3.7 Production and Characterization of nebulized mRNA-LNPs in PBS E % T80 (1:10) formulation 54

4 CONCLUSIONS AND FUTURE PERSPECTIVES 61

5 BIBLIOGRAPHY 65

List of Figures

Figure 1 Important discoveries and drugs approvals to reach mRNA therapeutics 3
Figure 2 A premature stop codon in image A stops translation originating a truncated protein of image B. To overcome this challenge a modified tRNA will bind to the premature stop codon which allows translation to continue as shown in image C. Adapted from [29]. 4
Figure 3 Different types of carriers for RNA delivery and their compositions 7
Figure 4 Next generation impactor left: A- 7-Stage apparatus; B- Induction Port; C- Pre-separator (does not apply to nebulizer testing) Right: 1- Bottom frame; 2- Support tray; 3- Lid with interstage 22
Figure 5 Microfluidics set up for LNPs production 26
Figure 6 A-Micromixer with air Bubbles; B-Micromixer accumulation after production 27
Figure 7 A-Dialysis set up; B- Dialysis cup with 1- dialysis device to place LNPs and 2- falcon to place the desired buffer 28
Figure 8 Nebulization set up, inside a closed box to contain the release of droplets to the surrounding environment, due to HSE concerns. 29
Figure 9 NGI set up for nebulized solutions inside an NGI cooler and a plastic bag for containment. 32
Figure 10 Delivered Dose set up for nebulized solutions using a jet nebulizer inside a plastic bag due to health, safety, and Environment (HSE) concerns [123]. 33
Figure 11 Microscope images of accumulated material (filaments) inside the micromixer 35
Figure 12 microscope comparison between a reference vibrating mesh nebulizer (A) and the vibrating mesh nebulizer used in the formulation development (B) with a magnification of 64X. 50
Figure 13 Gel electrophoresis comparison between RNA ladder and unencapsulated mRNA sample with SDS, microfluidic, dialysis, diluted dialysis, and three nebulization samples. 57

List of Tables

Table 1 Main advantages and disadvantages of different microchannels 12
Table 2 Advantages and disadvantages of the different types of nebulizers 16
Table 3 Cut-off diameter for NGI at flow rate 15 L/min 22
Table 4 List of reagents used with the respective supplier, purity, and Cas (Chemical Abstracts Service) number. ND: No data 25
Table 5 Encapsulation efficiency results on day 3 and day 100 of the stability test 39
Table 6 Osmolarity of two formulations after dialysis 44
Table 7 Osmolarity of formulation PBS with E % T80 and formulation on PBS with F % P188, after production, after dialysis and dilution, after nebulization 46
Table 8 Encapsulation efficiency of formulation PBS with E % T80 and formulation on PBS with F % P188, after production, after dialysis, dilution, and nebulization 47
Table 9 Values of MMAD, GSD, and FPF of nebulized solutions, determined with Copley CITDAS software.(n=1) 48
Table 10 Comparison between literature values and produced values of MMAD, GSD, and FPF for salbutamol molecule 49
Table 11 Encapsulation efficiencies of tRNA LNPs with PBS and E % T80 in a dilution ratio V/V 1:10 (n = 3) 51
Table 12 pH, zeta potential, and osmolarity results throughout all process steps 52
Table 13 Values of MMAD, GSD, and FPF for nebulization of formulation PBS with E % T80 (n = 2) 53
Table 14 Osmolarity comparison between mRNA LNPs and tRNA LNPs after dialysis, after dilution, and after nebulization 55
Table 15 Encapsulation efficiency of mRNA LNPs with formulation PBS with E % T80, dilution ratio 1:10, after microfluidics, after dialysis, after dilution, and after nebulization 56
Table 16 HPLC area of mRNA and impurity peaks of unencapsulated mRNA sample and microfluidic, diluted, and nebulization samples 56
Table 17 Values of MMAD, GSD, and FPF for Nebulization of mRNA and tRNA LNPs formulation with PBS and E % T80 59

List of graphics

Graph 1 Compilation of all batches of LNPs plotted against their particle size and PDI 36
Graph 2 tRNA LNP's particle size and PDI stability test for storage at room temperature (20-25 ºC), at 2-8 ºC, at -20 ºC, and freeze and thaw cycles. 37
Graph 3 Particle size and PDI comparison of different formulations after microfluidics, after dialysis, and after nebulization 40
Graph 4 Intensity particle size graphs from Malvern DTS v5.2 software after dialysis and after nebulization (n=3) 41
Graph 5 Particle Size and PDI of different formulations with PBS buffer after microfluidics LNPs production, after dialysis, and after nebulization, and comparison with two best formulations from Graph 3 42
Graph 6 Particle size and PDI comparison of screening formulation of PBS with different P188 concentrations after microfluidics, after dialysis, and after nebulization 43
Graph 7 Osmolarity dilution curve with LNPs in formulation with PBS 44
Graph 8 Particle size and PDI of diluted screening formulations after microfluidics, after dialysis with a dilution ratio of 1:10 (V/V), and after nebulization (n=3) 45
Graph 9 Particle size distribution (intensity) after nebulization in formulations with diluted ratio 1:10 V/V (n=3) 46
Graph 10 Mass deposition profile of NGI test for formulation PBS with F % P188 and PBS with E % T80 (n=1) 48
Graph 11 Comparison between the mass deposition profile for a salbutamol solution with a vibrating mesh nebulizer Innospire Go according to the literature (left) [120] and determined experimentally (right). 49
Graph 12 Particle size and PDI results of tRNA LNPs with PBS and E % T80 after microfluidics, after dialysis, after dilution, and after nebulization (n = 3). 51
Graph 13 Mass deposition profile of formulation with PBS and E % T80 in the different stages (n = 2) 52
Graph 14 Particle size and PDI comparison between formulations that encapsulates tRNA and mRNA after production, after dialysis, after dilution, and after nebulization 54
Graph 15 Mass distribution of mRNA LNPs formulation with PBS and E % T80 in the different stages of NGI 58

LIST OF EQUATIONS

Equation 1 Stokes-Einstein equation where d(H) is the hydrodynamic diameter, D is the translational diffusion coefficient, K is the Boltzmann's constant, T is the absolute temperature, and η is the viscosity of the solution. 18

Equation 2 Henry equation where z is the zeta potential, U_E is the electrophoretic mobility, ε is the dielectric constant, η is the viscosity, and f(Ka) is Henry's function where the values of 1,5 or 1,0 are generally used as an approximation 19

Equation 3 GSD determination based on mass cumulative curve points 22

Equation 4 Fine particle fraction determination, where Fine Particle Dose (FPD) is the mass of particles with an aerodynamic diameter smaller than 5 μm and the Delivered Dose (DD) is the total mass that is recovered from the NGI (with exception of the drug quantity that remains in the nebulizer). 23

Equation 5 Encapsulation Efficiency of Lipid Nanoparticles 31

ACRONYMS

Abbreviature	Name
ALAS1	AminolevuLinic Acid Synthase 1
aPSD	Aerodynamic Particle Size Distribution
ASO	Antisense Oligonucleotides
asRNA	Antisense RNA
BRS	Breathing Simulator
Cas	Chemical Abstracts Service
CQAs	Critical Quality Attributes
COPD	Chronic Obstructive Pulmonary Disease
DC-Chol	3 beta-[N-(N',N'-dimethylaminoethane)-carbamoyl]cholesterol
DLS	Dynamic Light Scattering
DMG-PEG 2000	1,2-dimyristoyl-rac-glycero-3-methoxypolyethylene glycol-2000
DOTAP	1,2-dioleoyl-3-trimethylammonium propane
DPI	Dry Power Inhalation
DSPC	Distearoylphosphatidylcholine
DUSA	Dosage Unit Sampling Apparatus
EDTA	Ethylenediaminetetraacetic acid
EE	Encapsulation Efficiency
EU	European Union
FIRS	Forum of International Respiratory Societies
FPF	Fine particle fraction
FRR	Flow Rate Ratio
GSD	Geometrical standard deviation
HSE	Health, Safety and environment
HFF	Hydrodynamic Flow Focusing
iRNA	interference RNA
IVT	In vitro Transcribed
JN	Jet Nebulizer
LDV	Laser Doppler Velocimetry
LNPs	Lipid Nanoparticles
miRNA	Micro RNA
MMAD	Mass median aerodynamic diameter
MOC	Micro-orifice collector
mRNA	Messenger RNA
NaCl	Sodium chloride
NGI	New Generation Impactor
P188	Poloxamer
PBS	Phosphate buffered Saline
PDI	Polydispersity index
PEI	Polyethyleneimine
pMDI	Pressurized Metered-Dose inhalation
PS	Pulmonary Surfactant
RISC	RNA-Induced silencing complex
RNA	Ribonucleic Acid
rRNA	Ribosomal RNA
SHM	Staggered Herringbone Micromixer
siRNA	Small interfering RNA

T80	Tween 80
TFR	Total Flow Rate
TrM	Toroidal Mixer
tRNA	Transference RNA
UN	Ultrasonic Nebulizer
USP	United States Pharmacopeia
VNM	Vibrating Mesh Nebulizer
WHO	World Health Organization

1 INTRODUCTION

1.1 Respiratory diseases and economic burden

The World Health Organization (WHO) presented a report in 2019 stating that respiratory diseases cause more than 8 million deaths annually. It is also mentioned that chronic obstructive respiratory diseases, lower respiratory infections, trachea, bronchus, and lung cancers, as well as tuberculosis, are 3rd, 4th, 6th, and 13th, respectively, in the top 20 world causes of death [1]. The Forum of International Respiratory Societies (FIRS) advised that it is essential to boost the funding for respiratory research, to improve its prevention and treatment [2].

In 2021, the global respiratory diseases drugs had a size market estimated at 142 billion dollars and it is estimated a growth to 292 billion dollars by 2026 [3]. It is estimated that the 27 countries of the European Union (EU) spend more than 380 billion euros every year on respiratory diseases, from which 55 billion is spent on hospital and drug costs [4].

Conventional therapeutic approaches are based on small drug molecules. Biologic drugs are larger and complex molecules produced with biotechnology that started having an increasing relevance in the last years − between 2015 and 2019 more than 25 % of the new drugs approved by the FDA were biologic drugs to treat a variety of diseases like asthma, cancer, genetic disorders, and allergies. An example of a biopharmaceutical used in the treatment of respiratory diseases is Mepolizumab, which in 2015 was the first biologic drug FDA-approved to target IL-5, helping in the treatment of severe asthma [5], [6].

With the exponential growth of biotechnological medications during the last three decades, biopharmaceuticals became an attractive pharmaceutical sector for companies and, in 2016, according to Standard & Poor's industry statistics, 48 % of the top 100 medications were biotechnology goods [7]. If we look at the growth of the mRNA market used for the treatment of diseases, it will increase from 46.7 billion dollars in 2021 to 101.3 billion dollars by 2026, representing an increasing tendency for this type of treatments [8].

The number of people suffering from respiratory diseases that can lead to death, combined with the attractive potential economic value of biological drugs, make the research and development of this type of drug to treat respiratory diseases an interesting market for pharmaceutical companies to invest in the next years.

1.2 RNA based therapies

Recent technological advances in producing RNA to be used as a therapy, has been improving, which, combined with the abovementioned benefits associated, has increased the investment interest, research, and development in this field. In this subchapter, it is important to reflect at the evolution of the knowledge about genetic therapy and understand the mechanisms of action of this type of therapy..

1.2.1 RNA-based therapies history

Since Rosalind Franklin, Maurice Wilkins, James Watson, and Francis Crick contribution to DNA double helix discovery in 1953 (Figure 1), it was very relevant to know how DNA could produce proteins [9]. The answer was found by Sydney Brenner, François Jacob, Jim Watson, and his colleagues with the discovery of messenger RNA (mRNA) in 1961 [10]. The mRNA, transfer RNA (tRNA), and ribosomal RNA (rRNA) constitute the three main RNA types and they are responsible for transporting the genetic information from the DNA in the nucleus to the machinery that makes the proteins [11]. This discovery allowed the development of new treatment approaches based on protein encoding, where antisense RNA (asRNA) or messenger RNA (mRNA) are some examples of these new approaches.

asRNA is a synthetic oligonucleotide that will link to the complementary base pair of the RNA target which inhibits RNA translation. On the other hand, mRNA will encode a sequence for a specific protein that is either being produced with a defect, is absent, or creating antigen proteins [12]. In this way, the mRNA technology was designed to transfer genetic information into the cytoplasm of the cell, which in turn can help prevent or treat certain diseases [13].

In 1978, Mary Stephenson and Paul Zamecnik developed one of the first experiences with oligonucleotides to inhibit the Rous sarcoma viral RNA translation [14], [15].

It was only in 1990 that the first mRNA therapy approach was published by Wolf, Malone, and Williams, from the department of pediatrics and genetics in Wisconsin University, where genetic information was transferred to mice to understand if mRNA retained protein expression when injected [16]. Due to its lower stability in comparison with DNA, various studies started to try to improve the stability and immunogenicity of *in vitro*-transcribed (IVT) mRNA [17], [18].

Almost twenty years after the first RNA experience, in 1998, the first asRNA drug, Fomivirsen, was approved to treat a viral infection, cytomegalovirus retinitis. The goal of this drug was to link to the complementary sequence of mRNA produced by the cytomegalovirus to inhibit its replication [19].

In 2018 and 2019, the two first Small interfering RNA (SiRNA) drugs were approved, Patisiran and Givosiran. Patisiran is a drug that helps in transthyretin amyloidosis, a hereditary liver disease, by decreasing the transthyretin protein-encoding [20]. Givosiran is a drug that treats acute hepatic porphyria (AHP) by gene silencing of aminolevulinic acid synthase 1 (ALAS1) [21].

With the appearance of covid-19 world pandemic and the necessity to create a fast and secure vaccine, the first mRNA vaccines appeared on the market, the Moderna vaccine and the Pfizer/ BioNTech vaccine. This fast development of vaccines with mRNA technology increased RNA knowledge in a short time and opened the opportunity to use the same technology in other diseases [12].

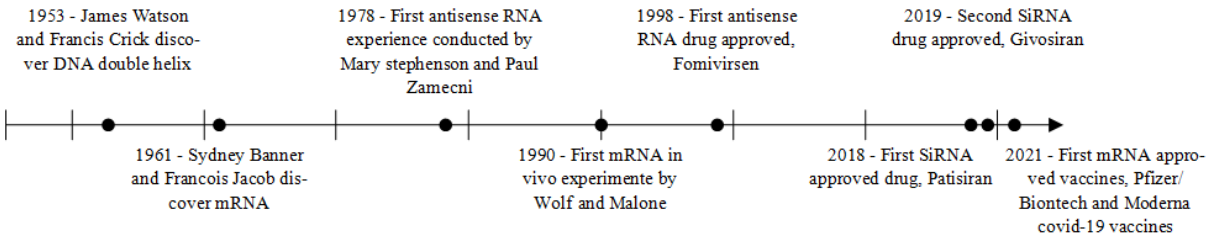

Figure 1 Important discoveries and drugs approvals to reach mRNA therapeutics

1.2.2 RNA therapeutics

RNA can have three potential therapeutic effects: inhibition of gene expression, protein-encoding, and protein targeting, depending on which type of RNA is used [22].

Inhibition of gene expression occurs when a short RNA strand binds to a specific mRNA molecule, which blocks mRNA translation into proteins. This can be done through Antisense Oligonucleotides (ASO) that pairs with mRNA-activating RNase that destroys the mRNA. MicroRNA (miRNA) or Small Interfering RNA (siRNA) are short RNA strands with a similar function to ASO, that are coupled to argonaut protein and other proteins, which results in the RNA-induced Silencing Complex (RISC). RISC will bind to a target mRNA and break it, conducting mRNA to degradation before transformation in proteins [23], [24].

mRNA can be used as a therapy by encoding for a specific protein (for example a target antigen) to create an immune response. RNA aptamers are RNA oligonucleotides that bind to a specific target with high affinity and specificity, acting in a similar mode to antibodies, that can be used to

inhibit the expression of target proteins. Due to their synthetic origin, they are usually called chemical antibodies [23].

In the last years, a revolutionary RNA approach has been starting to take shape − the transfer RNA (tRNA) based therapeutics. tRNA is responsible for the translation of mRNA into a specific amino acid [25]. The tRNA has the amino acid which is referred to in one end, and the anticodon present on the other end of the chain. When tRNA binds the correspondent mRNA codon to its anticodon, the translation of the codon to the amino acid occurs. The ordered translation of mRNA codons will code a set of amino acids that will be a fully functional protein [26].

mRNA has specific codons to start and end the translation, but sometimes due to mutations, the translation can end prematurely, which originates proteins that will not function properly. More than 4 % of all genetic diseases occur due to these mutations, which can be corrected with a tRNA therapeutic. In this case, the tRNA will translate the defective codon, which was turned into a premature stop codon, into the correct amino acid, allowing it to produce the correct protein, as observed in Figure 2 [27]. Companies like Alltrna are now developing a tRNA therapy platform [28].

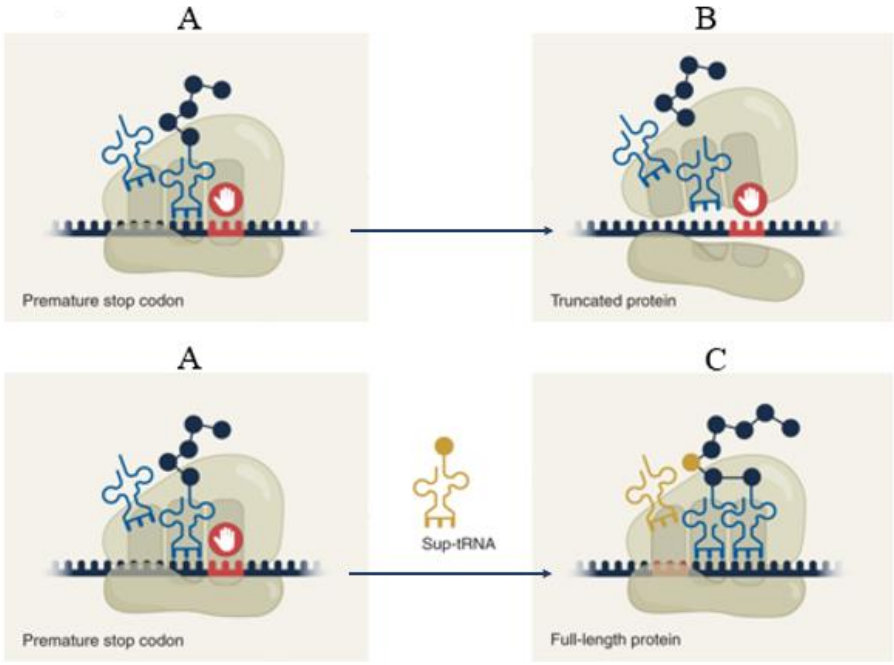

Figure 2 A premature stop codon in image A stops translation originating a truncated protein of image B. To overcome this challenge a modified tRNA will bind to the premature stop codon which allows translation to continue as shown in image C. Adapted from [29].

1.3 Challenges of RNA delivery

With such a variety of RNA therapeutics under development, it is important to understand the viability of delivery of the drugs into the target cells without being degraded during its administration. This challenge is considered one of the major barriers to RNA therapeutics development.

Since the present work is focused on inhalation, it will be discussed below the different delivery barriers in inhalation, how it is possible to overcome these challenges and the composition of the carriers that have shown to successfully deliver RNA into the lungs without compromising its integrity.

1.3.1 Delivery barriers

Inhaled pharmaceutics target the lungs for drug delivery, and the main goal is to reach epithelial cells. Upon inhalation, RNA needs to cross the nasal cavity, the pharynx, the trachea, and the highly-branched lung structure until reaching the target [6].

Therefore, the aerodynamic diameter is an important parameter that determines efficient deposition in the chosen targets since particles with different dimensions settle in different sites of the respiratory tract. Particles with sizes between 1 and 5 μm are considered inhalable particles since they can deposit in the lower respiratory tract, while sizes larger than 5 μm settle in the superior airway wall in bifurcations, and sizes lower than 1 μm are exhausted by normal breathing.

When inhalable particles settle in the lung, epithelium absorption is a physical boundary necessary to overcome to achieve the bloodstream. Particles can flow through the epithelium in two ways, paracellular transport or transcytosis [6]. If the particles do not have specialized receptors in lung epithelial cells, they are transported by paracellular transport, otherwise, active transportation is mediated by receptor-mediated transcytosis for particles that permeate actively the alveolar epithelium. After absorption, in the bloodstream, drugs are subjected to many types of proteases and peptidases which can degrade the RNA before reaching the target cells [6].

Inhalation of RNA therapies without any protection mechanism in the molecule of interest is extremely difficult since it is a hydrophilic molecule with a negative charge, therefore permeating the hydrophobic membrane is not possible. During the administration trajectory, if the fragile RNA molecule is not protected, its activity can also be compromised by RNases, an abundant nuclease that degrades RNA in the body [22].

With all these barriers which can compromise RNA therapy delivery, it is necessary to create a protective vehicle for the RNA, but safe for human inhalation, to facilitate its transport and release into the target cells without degradation during its journey.

1.3.2 RNA delivery strategies in inhalation

In recent years, many studies have focused on producing a safe carrier for RNA to get into target cells without being degraded. Lipid-based vectors, polymer-based vectors, and hybrid-based vectors are the three main types of carriers highlighted below.

Lipid-based vectors are popular RNA carriers and some of these carriers are already approved by the FDA for use in vaccines, like Onpattro, the first lipid nanoparticles (LNPs) drug carrier approved in 2018, or Doxil, the first liposome-based drug approved in 1995 [33], [34]. Liposomes (Figure 3 A) are formed by a phospholipid bilayer that encloses an aqueous solution containing RNA. They are often used as drug carriers because of their high delivery efficiency, good biodegradability, and easy formulation [35], [36]. The principal concern in liposomes is the use of cationic lipids, which enables better encapsulation but are associated with rapid clearance and toxicity concerns [36]. For that reason, LNPs (Figure 3 D), which use ionizable lipids instead of cationic lipids, are preferred for RNA delivery. LNPs are closed to liposomes, but the phospholipid layer is composed of other components, such as helper lipids and cholesterol to mitigate potential cytotoxicity. Their small size makes them preferred for inhalation via nebulization or dry powder inhalation (DPI).

Polymer-based vectors are recent carriers with fewer studies than lipid-based vectors, which bind cationic polymers to RNA through electrostatic interactions. These interactions can form polyplexes or micelleplexes. The usual polyplex (Figure 3 B) for RNA delivery is polyethyleneimine (PEI), which can have a high molecular weight and can be useful for delivering heavy and complex molecules [36]. The challenge of polymer carriers is their possible toxicity due to cationic polymers with a high degree of branching and molecular weight. Micelleplexes (Figure 3 E) are like polyplexes, but they can combine a drug and RNA delivery at the same time [37].

On the other hand, hybrid-based vectors overcome the limitations of the previous two carrier types by combining them into one new type of carrier [22]. The combination of lipid-based vectors with polymer-based vectors originated the lipopolyplexes and the cationic nanoemulsions. Lipopolyplexes (Figure 3 C) are formed from a nucleic acid-polycation complex core encapsulated in a lipid shell, combining the high stability and low cytotoxicity of lipid-based vectors with small particle size, endosomal escape, and high transfection activity advantages from the polyplexes. Another hybrid vector created was the cationic nanoemulsions (Figure 3 F), which is an oil-in-water emulsion that is being developed by Novartis using their adjuvant MF59 and is already proven to be clinically safe for children, adults, and elderly people [36], [38].

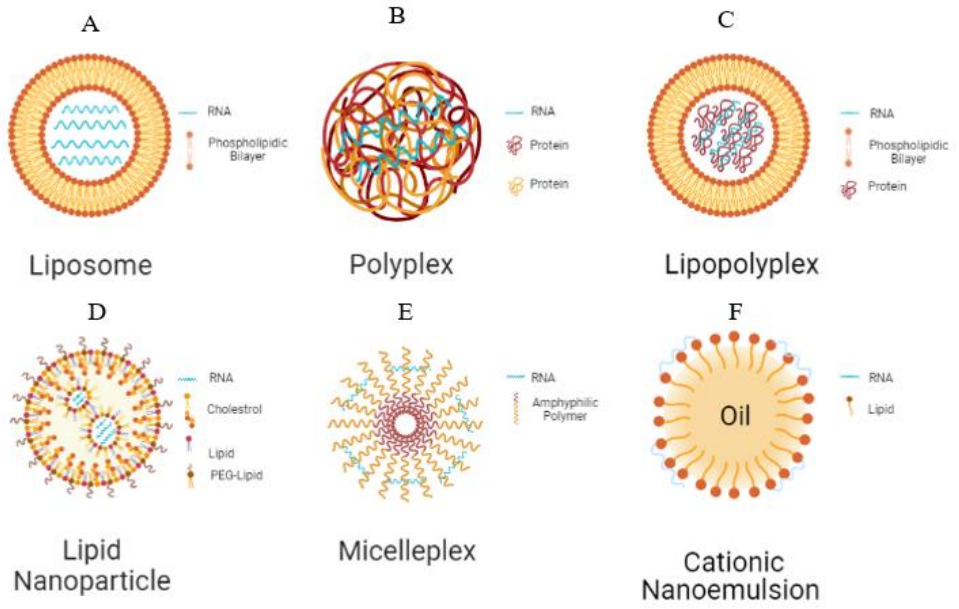

Figure 3 Different types of carriers for RNA delivery and their compositions

From the carriers talked about previously, LNPs are the most promising to encapsulate RNA, and had already been approved for use in covid-19 vaccines by Pfizer and Moderna, thus these carriers were selected for conducting the experimental work encompassed in this thesis. For that reason, it will now be discussed the composition and the role of each compound in the LNPs.

1.3.3 Lipid nanoparticle composition

Lipid nanoparticles are formed mainly of four components: cationic lipids (can be substituted by ionizable lipids), phospholipids, cholesterol, and PEGylated lipids [39]. Each component and its optimized ratios dictate the nanoparticle's desirable characteristics: high encapsulation efficiency, good structural integrity, good fusogenicity, good steric barrier effect, and easy endosomal escape.

Cationic lipids are important in improving encapsulation efficiency since their positive charge allows electrostatic interactions with RNA [49]. These lipids have been recently substituted by ionizable lipids, which in acidic conditions present a positive charge and with physiological pH present a neutral charge. Alteration of charge due to alteration of pH is an improvement in the nanoparticle capacity of RNA delivery since it promotes better intracellular delivery and higher clearance time in blood current due to neutral charge. At the same time, neutral charge ameliorates tolerability and pharmacokinetic properties in comparison with cationic lipids. The endosomal escape is also enhanced with ionizable lipids since, inside the nanoparticle with an acidic pH, the ionizable charge changes to

positive, which contributes to merging the lipid nanoparticle with the endosomal membrane allowing RNA to be released into the cytoplasm [39], [40].

Phospholipids are considered helper lipids, a group of lipids whose function is to enhance nanoparticle stability and promote phospholipidic bilayer destabilization for efficient nucleic acid delivery [39]. Usually, LNPs are made with one of the following types of phospholipids: phosphatidylcholines, like distearoylphosphatidylcholine (DSPC) or dioleoylphosphatidylcholine (DOPC), or phosphoethanolamine like 1, 2-dioleoyl-sn-glycero-3-phosphoethanolamine (DOPE). Phosphatidylcholines have cylindrical geometry making them the natural components in phospholipidic bilayer construction [41]. In the cases where it is beneficial to have destabilization in endosomal membranes to facilitate the endosomal escape, DOPE should be considered [42]. On the other hand, if it is more important to ensure the stability of the LNPs membrane, DSPC should be considered, although it might be a difficult endosomal escape since LNPs high stability could reduce its ability to release the RNA inside its core. One way to overcome the issue is using DOPC, which makes the LNPs more fluidized, but the drawback is that increasing fluidization in nanoparticles makes them more prone to opsonization [39].

Cholesterol is another helper lipid commonly used in LNPs formulation, due to its capacity to bind to empty spaces in the phospholipidic bilayer, making them more stable[41]. When LNPs are formulated with phosphatidylcholines and cholesterol, they promote a stable lipid bilayer [43]. It has been demonstrated that these can also promote membrane fusion [44]. At the same time, a study proved that cholesterol has low solubility inside the nanoparticle core, therefore it will accumulate on the nanoparticle surface, which destabilizes the phospholipidic bilayer and promotes endosomal escape [45], [46].

The PEG lipids are composed of a hydrophilic PEG molecule that is linked to a lipid chain. The hydrophobic part is attached to the LNPs bilayer, and the hydrophilic part stays on the LNPs surface [39]. The addition of PEGylation to LNPs reduces toxicity and at the same time increases half-time blood circulation, which leads to an accumulation of LNPs in diseased sites instead of the liver [47]. The steric barrier effect caused by PEGylation also prevents the aggregation of nanoparticles during production, which promotes a homogenous LNPs size between 50 and 100 nm, leading to a small polydispersity index[39], [47], [48]. Although PEGylation has many advantages, the quantity in each nanoparticle should be controlled and kept at a minimum value because high quantities promote LNPs fusion with the endosomal membrane, which represents a barrier in drug delivery [48]. The PEG size itself is important since it was demonstrated that small PEG size diffuses away from LNPs faster than large PEG size molecules, increasing the blood circulation time [50].

1.3.4 Importance of excipients

Pharmaceutical excipients are pharmacologically inert substances that are added to drugs, to ensure drug physical and chemical stability, bioavailability, biocompatibility, delivery to the desired target, and increase the drug quantity available for cell absorption [51].

The main objective of encapsulating RNA into LNPs is to reach the target cell. The composition of each lipid in the LNPs should be carefully determined since, as reported in subchapter 1.3.3, higher concentrations of some lipids can promote toxicity.

For inhalation proposes, the excipients already approved for use by the FDA are very limited due to the limited guidance available for the potential use of excipients available from other industries or already used in different applications, for example from parenteral route to inhalation route [52].

Nebulization solutions are usually composed of drugs dissolved in aqueous isotonic solvent systems that can contain other preservative excipients that have functions to decrease the possibility of microbial growth, being utilized as buffers, osmolytes, or cryoprotectants [53]. In LNPs, nebulization excipients added should not only have into account solution stability but also LNPs stability and the dispersion capacity of the solution when nebulized.

Buffering agents like Phosphate Buffered Saline (PBS) are frequently used in this type of solution since it helps to adjust the osmolarity of the solution and are capable to maintain the pH stable when formulations are frozen for storage [54], [55].

Another class of excipients widely used in nebulization solutions is surfactants, like polysorbates and sorbitanes since they are reported as capable of increasing dispersion or dissolution of the drugs when nebulized and can present concentrations from 0.001 to 2 % (W/V). Surfactants also modify surface properties, which enables modulation of the aerodynamic performance of the solution and aerosolized droplets. For biological formulations, surfactants are also used to prevent aggregates, which for systems like LNPs is of great importance, since when LNPs pass through the nebulizer mesh the vibration that promotes this passage can lead to nanoparticle aggregation and/or fusion [54], [56], [57].

Excipients with cryoprotectant function are very important for long-stability storage. Usually, these excipients are sugars like mannitol, trehalose, sucrose, or glucose and are widely used in the freeze-drying process. In the present system, this type of excipient would help prevent aggregation and maintain stability if the samples are stored at freezing temperatures [57] – [60].

1.4 Lipid nanoparticles production

LNPs encapsulating RNA require a production process that allows high control during production and promotes high RNA entrapment efficiency and reproducibility. In the following subchapter, some of the existent LNPs process methods will be discussed, followed by an exhaustive examination of the microfluidics ethanol injection method, which will be used for producing LNPs in the thesis, and some parameters which are important to have a controlled microfluidic production.

1.4.1 LNPs production methods

Most RNA-LNPs production methods are performed using rapid mixing methods, which consist of mixing a fluid stream that contains lipids in an organic phase with another fluid stream that contains RNA in an aqueous phase. When the two streams encounter, the dilution of the organic phase in the aqueous phase occurs, promoting the production of LNPs, since the lipids are hydrophobic and tend to form spherical particles to reduce interfacial tension, which encapsulates RNA in the aqueous solution [61].

In rapid mixing, two methods had been widely used for LNPs production: 1) lipid-film hydration followed by extrusion or sonication homogenization, and 2) ethanol injection.

Liposome-based products are formed through a lipid-film hydration technique where the lipid film is dried to evaporate the organic solvent. Then the aqueous phase is added to the lipid film, promoting the self-assembly of multilamellar vesicles with several lipid layers, containing inside its core the aqueous phase. Several freeze-thaw cycles can be performed to achieve liposomes with fewer lipid layers and a higher volume of aqueous phase encapsulated in its core. Since the liposomes produced have a broad particle size distribution, several extrusion cycles or sonication cycles are then performed to homogenize the liposome's particle size. [62], [63]. LNPs have also been produced by lipid-film hydration, but due to multiple production steps and lower encapsulation efficiencies, it is not considered a preferable method [40], [61] – [63].

The ethanol ejection method appeared to overcome the problems inherent to the lipid film hydration method [40]. The method consists of a lipid solution with ethanol mixed in a micromixer with an aqueous buffer system with RNA, generating “precipitates” that are nanoparticles with RNA inside them [64]. The nanoparticle size is dependent on a wide range of factors, like lipid concentration, choice of lipids, flow rate ratio (FRR), or total flow rate (TFR), which can be controlled. In comparison with the previous method, the principal advantage is the simplicity, absence of harmful chemicals and physical treatments, and the possibility of scale-up [64]. The application of this technology has advantages such as using always a controlled laminar flow with a Reynolds number usually lower than

100, low energy consumption, small diffusion distances, and a better ratio surface of area/volume. As an economic advantage, less demand for materials makes the technology cheaper [65]. For these reasons, the ethanol-injection method was adopted for RNA-LNPs production during the thesis.

1.4.2 Ethanol injection method, and operational process parameters

In 1973, Batzri and Korn developed the ethanol injection method as an improved alternative to the thin film hydration method combined with sonication [66]. The method combines lipids in ethanol with RNA in an aqueous phase. The fast ethanol dilution in the aqueous buffer promotes the self-assembly of lipid vesicles due to a rise in the solvent's polarity, which promotes a homogeneous solution with nanoparticles [67].

The working principle of this method relies on the good mixing of the two phases. With the evolution of technology, different types of micromixers have started to appear to continuously improve the mixing with higher throughput in mind, where it can be highlighted the Hydrodynamic Flow Focusing micromixer (HFF), the Staggered Herringbone Micromixer (SHM) and the Toroidal Mixer (TrM).

Hydrodynamic Flow Focusing micromixer (HFF) is one of the most used micromixers, where an organic phase channel containing lipids will join an aqueous phase channel containing RNA and form the LNPs in the liquid-liquid interface [68], [69]. This micromixer can be a 2D HFF, which has horizontal channels for interface mixing, or 3D HFF which has a cylindrical interface mixing, increasing the mixing time and consequently the LNPs production [69]. The limited flow rate is the main disadvantage of HFF, making it difficult for the scale-up process and hard to achieve high throughput [65].

To overcome the HFF problems, chaotic advection micromixers were created, which consist in inserting barriers inside the microchannels, since promoting chaos is an efficient way of mixing streams with a low Reynolds Number [65], [70]. A staggered Herringbone Micromixer (SHM) is a usual chaotic advection micromixer with transverse components inside the microchannel, improving mixing due to chaotic flow and consequently decreasing mixing length [69]. This design can work with higher flow rates than HFF, can be scaled up, has an encapsulation efficiency higher than 90 %, and generates nanoparticles with a size lower than 100 nm, being a perfect technique for laboratory work [63], [65], [69] – [71].

Flow rate capacity in SHM continues to be a problem, although recently Precision Nanosystems Inc. has developed a novel channel capable of eliminating that problem, the Toroidal Mixer (TrM)[69]. This method can produce higher mixing efficiency in laminar flow due to circular structures allowing to create a chaotic mixing in flow rates up to 20 L/h [72]. In comparison with SHM, it

seems to be a promising technology, but with low research yet, SHM stands as the best continuous flow process for LNPs production.

Table 1 summarizes the main advantages and disadvantages of micromixers.

After choosing the right micromixer, other operational parameters that can affect LNPs morphology should be considered, where the most critical are N/P ratio, Total flow rate (TFR), Flow rate ratio (FRR), and lipid concentrations.

Nitrogen to phosphate ratio (N/P) is an important operational parameter in microfluidics since it describes the interaction between the amino group present in ionizable lipid and the phosphate present in RNA, responsible for the complexation of RNA with the LNPs. This ratio can have an impact on particle size, as it was reported that increasing the N/P ratio will decrease LNPs size since there is less RNA to encapsulate in each LNPs [73] and can also have an impact on mRNA expression, as studies show that N/P higher than 15:1 will promote a reduction in protein expression [74]. The delicate balance between good protein expression and small particle size makes different companies choose different N/P ratios, for example, Patisiran encapsulates SiRNA with an N/P ratio of 3 while mRNA LNPs vaccines use an N/P ratio of 6 [53].

Table 1 Main advantages and disadvantages of different microchannels

Micromixer type	Advantages	Disadvantages	Micromixer diagram	Bibliography
Microfluidic Hydrodynamic Flow Focusing (HFF)	• Smaller molecules (lower than 150 nm) • Higher encapsulation Efficiency (20 higher than BE) • No need for post-processing treatments	• Diluted sample concentration • Limited flow rate production	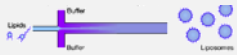	[63], [65], [68], [69]
Microfluidic Staggered Herringbone Micromixer (SHM)	• Chaotic advection mixing • High encapsulation efficiency (90 %) • Small molecules (lower than 100 nm) • Available for scale-up • Homogeneous particle size	• More expensive • Limited flow production		[63], [65], [69] – [71]
Toroidal Mixer (TrM)	• Chaotic advection mixing • High encapsulation efficiency (90 %) • Small molecules (lower than 100 nm) • Possible to have a high flow rate (up to 20 L/h)	• Recent approach with low publications		[69]

The total flow Rate (TFR) and Flow Rate ratio (FRR) between the aqueous phase and lipid phase are also important to control LNPs size. A study reported that varying TFR from 5 - 20 mL/min in an SHM micromixer concluded that increasing TFR reduces LNPs size, but for TFR higher than 10 mL/min no significant size changes were reported. In the same study, it was concluded that changing FRR from 1:1 to 5:1 decreases particle size, and while 1:1 presented a high particle size (between 200 nm and 800 nm), 3:1 and 5:1 ratio presented a stable particle size between 37 and 65 nm [40]. Similar conclusions were presented in SiRNA LNPs productions with SiRNA/Lipid ratio of 0.06 (W/W) and TFR changing from 0.02 to 4 mL/min [75]. Literature demonstrated that lipid concentration was also important for particle size control since changing concentration from 5 to 20 mg/mL promoted particle size increase [76].

1.5 Inhalation methods

From the different administration routes available to treat respiratory diseases, the inhalation route is preferable since direct drug delivery into the active site presents as advantages lower systemic side effects, smaller drug volumes used, and consequently smaller treatment times. Despite this, the irritation of the airways may stimulate the cough reflex and the necessity of a correct inhaler technique for maximum drug delivery, are the major drawbacks of this technology [78].

Regarding the delivery of nanoparticles through the inhalation route, there are three possible devices already on the market that are suitable for LNPs delivery: pressurized metered-dose inhalers, dry powder inhalers, and nebulizers.

1.5.1 Pressurized Metered-Dose inhaler (pMDI) Dry Powder Inhaler (DPI)

The pressurized metered-dose inhaler (pMDI) is a portable device with a metal can that when pressed, the valve opens and the liquid is released into the actuator and transformed into small droplets in a precise quantity of drug that will reach the patient lungs [6], [79], [80]. The pMDI is the primary choice for the treatment of respiratory diseases such as asthma and COPD [81], and the continuous success of pMDI is related to the fact of being a portable device, user-friendly, and without any previous preparation before the treatment. Although the uses of CFCs as a propellant, the high pharyngeal deposition, and the coordination between pressing the actuator and inhalation promoted the novel inhalation methods' appearance [82], [83].

Dry powder inhalers (DPI), appeared in the market to solve the patient coordination problems associated with pMDI, eliminate the use of CFCs as propellants, and increase drug stability in comparison with liquid solutions. DPI delivers an aerosolized drug powder with sizes between 1 and 5 μm with some excipients like lactose, mannitol, sucrose, trehalose, sorbitol, or glucose [81], [84]. The complex process of drying the liquid solution into a powder and the air humidity effect in the particle de-aggregation are some challenges associated with DPI drug production and delivery [81].

1.5.2 Nebulization: different types and comparison with previous methods

Nebulization consists of the conversion of a liquid by a mechanic or thermal process into aerosol droplets to be inhaled and deposited in the patient's lungs [86]. These devices are indicated for patients with difficulties in the use of the previous devices, such as babies, children, the elderly, or patients with severe diseases that have mobility and coordination issues [87].

Compared with dry-powder formulations, nebulization delivers high amounts of drug solutions with higher efficiency, and it is simpler to formulate and produce, which makes this a highly cost-effective product [88]. Also, the low investment associated with this technology, makes nebulizers one of the first steps in the development of inhalable formulations.

Since the first nebulizer was made in 1858 by Jean Sales-Girons, the technology has been improved and nowadays there are four main types of nebulizers already on the market: Jet Nebulizers (JN), Ultrasonic Nebulizers (UN), Soft Mist Nebulizer (SMN) Vibrating Mesh Nebulizers (VMN) [89].

Jet nebulizers were the first nebulizers commercially available in the 1930s, and nowadays they are the most common type of nebulizers on the market. The working principle is based on the Bernoulli Principle which states that, in a closed circuit, energy is conserved, thus if the fluid velocity increases with the decreasing size of pipe diameter, there is a pressure drop in tangential or coaxial flow pipes, leading to a suction effect called Venturi effect [90]. These pieces of equipment blow compressed air into a small diameter pipe, originating a low-pressure area around the liquid reservoir, which will suck the liquid into the airstream and then shatter it into small aerosol droplets. For efficient droplet delivery, the solutions used should have a viscosity between 1 and 6 cP [91]. The baffle presented in the airflow outlet will help the liquid to be shattered and enable the small droplets to go to the patient's lungs while the larger droplets settle in the liquid reservoir and will be nebulized again. JN will shatter some particles more than once, which presents a big disadvantage for biological drugs since liquid shattering causes shear stress in the particles. This repeated stress in fragile particles, like LNPs-mRNA, can break them, releasing mRNA earlier than intended and leading to the degradation of mRNA by RNases presented in the body before reaching the target [88], [92]. Another disadvantage

presented by jet nebulizers is the large residual volume remaining at the end of nebulization, between 1 and 1.5 mL, which for expensive biological nanoparticle drugs presents a major economical drawback [93].

Ultrasonic nebulizers have been used since the 60s, but due to large residual volumes, inability to aerosolize viscous solutions, and degradation of heat-sensitive materials these types of nebulizers are not the most widely used [94]. The piezoelectric crystal inside the nebulizer converts electric signals to mechanical movements, creating an oscillatory movement with frequencies around 20 KHz. The movement in the liquid reservoir creates superficial waves that will promote droplet formation, which are dragged by the airflow [91]. The droplets can be formed by two methods, cavitation, or capillary. In cavitation, these mechanical movements create low-pressure areas which promote vapor bubbles formation. Then the oscillatory movements break the bubbles and destabilize the liquid surface, leading to droplet creation. On the other hand, capillary waves promote liquid surface waves until reaching a point where they collapse [94]. The droplet's size is inversely proportional to two-thirds of the acoustic power frequency and to nebulize the solution, the formulation viscosity should stay below 6 cP [91], [95]. For biological drugs, this type of nebulization is not suitable since the increasing temperature up to an additional 10 ºC after 5-10 min of nebulization can denature the mRNA [91], [92].

In 1993, the company Omron put on the market the first ultrasonic vibrating mesh nebulizer, a piece of revolutionary nebulization equipment based on the same principle of ultrasonic nebulizers. The vibrating mesh nebulizer uses the piezoelectric transducer to vibrate a perforated mesh to generate the droplets. This process is based on a pressure change before the mesh membrane that will make the liquid solution pass through the mesh and create small liquid droplets, all of a similar size, making the baffles unnecessary in this configuration [94], [96]. Rayleigh's theory predicts that the droplet size will be approximately two times the size of the mesh hole [93]. This type of nebulization is characterized by only a single passage through the mesh, which reduces the particle shear stress, low wasted volume, and fast treatment time. It has not been reported an increase in the temperature during nebulization, making it the preferable nebulizer for biological drugs like the LNPs-RNA system [93]. The main disadvantage is the careful cleaning of the mesh to avoid clogging the orifices and future bacterial contamination [92], [94].

Soft mist nebulizers are the most recent nebulizers in the market, they entered the European market in 2004 to substitute the pMDI, which still used chlorofluorocarbons. These devices combine a variety of principles used in other nebulizers to achieve high lung deposition in deep parts of the lungs. Table 2 summarizes the different advantages and disadvantages of each nebulizer type.

Since this thesis will work with sensitive biological drugs the most appropriate nebulizer available is the vibrating mesh nebulizer [98].

Table 2 Advantages and disadvantages of the different types of nebulizers

Nebulizer	Advantages	Disadvantages	Bibliography
Jet Nebulizer	• Aerolize different types of liquid (solutions, suspensions, oils …) • Effective delivering drugs that cannot be delivered with pMDIs or DPIs • Cheaper technology	• Long treatment times (> 6-15 min) • Large residual volume (1-1.5 ml) • Not suitable for biologic drugs due to high mechanical stress caused by the process	[88], [89], [91] – [93]
Ultrasonic Nebulizer	• More efficient than JN • Shorter nebulization time • Better for large volumes	• Inability to aerolize viscous solutions • Degradation of drugs that are heat-sensitive	[89], [91], [92], [94]
Soft Mist Nebulizer	• ---	• High lung deposition (> 50 %) • Can achieve deep lung deposition	[98]
Vibrating Mesh Nebulizer	• Low residual volume (0.1-1.25 ml) • Low mechanical stress during nebulization process • More silent than jet nebulizer • Easy to use	• Limited in delivery of suspensions • Some models are available only for a specific drug • Potential loss of performance due to the inadequate cleaning regime	[89], [92] – [94]

1.6 Quality attributes for inhaled RNA-LNPs

To guarantee that the LNPs are safe for human use, it is necessary to evaluate how particles behave throughout the production process, with characterization tests done when nanoparticles are produced, dialyzed, and nebulized. For that reason, critical quality attributes (CQA) are defined, which are physical, chemical, biological, or microbiological properties or characteristics that should be within an appropriate limit, range, or distribution to ensure the desired drug quality [99]. Here two types of CQAs should be defined, the CQAs related to LNPs and the CQAs related to the Inhalation method.

In LNPs CQAs are Important for determining their *in vivo and in vitro* performance, where LNPs size, polydispersity, surface charge, PH, osmolarity, RNA encapsulation, lipid, and RNA content are some important CQAs referred in literature [73], [99].

Before the formulation approval, it is necessary to characterize its performance when nebulized, where defined CQAs are the delivered dose, which is the amount of drug that is emitted from the device available for later use, and the aerodynamic particle size distribution that determines the quantity of emitted dose that reach the lungs or nasal mucosa during device actuation [100].

The next subchapters will address the characterization methods used to address each CQA and their importance to ensure LNPs, RNA, and final drug product quality.

1.6.1 Particle Size

The particle size of the LNPs determines the success of the formulation, and it should have a homogeneous size distribution, reflected by the polydispersity index with dimensions that should stay smaller than 200 nm to avoid uptake by cells of the RES and larger than 10 nm to avoid renal clearance [101], [102].

Dynamic light scattering (DLS) is a method where the particle size diameter is measured according to its Brownian motion, defined as the movement of particles in a liquid due to collisions with the molecules that surround them. The particle movement inside the liquid matrix is random and their velocity allows to determine their size. The principle considers that smaller particles move faster than larger ones.

The continuous light scattering by the irradiated particles allows an understanding of their movement, which enables the calculation of particle velocity and, consequently, an average particle size, using the Stokes-Einstein equation.

$$d(H) = \frac{KT}{3\pi\eta D}$$

Equation 1 Stokes-Einstein equation where d(H) is the hydrodynamic diameter, D is the translational diffusion coefficient, K is the Boltzmann's constant, T is the absolute temperature, and η is the viscosity of the solution.

DLS will provide a graph where it is showed the intensity in the function of the size diameter and, at the same time, a polydispersity index (PDI) can be calculated. The calculated polydispersity index (PDI) measures the degree of non-uniformity in the particles' size population. PDI values below 0.3 indicate that the particle size of the population is homogeneous, whereas values higher than 0.3 indicate a higher range of sizes in the sample [103].

1.6.2 Surface Charge

The surface charge can promote or difficult cellular uptake since if a particle has a positive charge it can pass through the cell membrane and reach the cytoplasm in an easier way than negative charge particles. The charge value cannot be high otherwise it will penetrate easily into the cells and can cause cytotoxic effects [104]. For clinical purposes, LNPs should present a neutral zeta potential [73], [105].

LNPs suspended in the solution usually have a charge, and if that charge is opposite to the particle charge, then a migratory movement of anions or cations occurs in the direction of the particle surface. This originates a diffuse layer where ions closer to the particle surface are strongly linked and further ions are weakly linked to the particle. Another layer called the slipping layer is the layer that divides the ions still affected by the particle charge from the ones that are not affected. The energy potential in the slipping layer is called zeta potential.

The surface charge is measured by Zeta potential analysis, which is determined by calculating the electrophoretic mobility, using a Laser Doppler Velocimetry (LDV) to measure the velocity of the particle when an electrical field is applied, and then applying the Henry equation (Equation 2).

$$U_E = \frac{2\varepsilon z f(Ka)}{3\eta}$$

Equation 2 Henry equation where z is the zeta potential, U_E is the electrophoretic mobility, ε is the dielectric constant, η is the viscosity, and f(Ka) is Henry's function where the values of 1,5 or 1,0 are generally used as an approximation

pH is an important parameter to have into account during these measurements since pH affects the zeta potential [103].

1.6.3 Osmolarity

Osmolality is the number of solute particles dissolved in a solvent and is an international requirement for pharmaceutical solutions as reported in USP <785> [107]. Plasma in the bloodstream usually has an osmolarity ranging from 300-310 mOsm, which should be the target for pharmaceutical solutions, to avoid swelling or contraction of the tissues with which they come in contact. It is reported that for intravenous administration, solutions up to 450 mOsm/Kg are well tolerated [106].

Osmolarity is the difference between the freezing point of pure water and the freezing point of the aqueous solution sample, measured using an osmometer [108]. The equipment will reduce the temperature of the aqueous solution at the supercooling point, which is the temperature below the freezing point, but where the solution remains in the liquid state without stirring. Then, when the solution is stirred, freezing is initiated, and the temperature at which solution freezing occurs is measured [109].

1.6.4 pH

Neutral pH is an international requirement for pharmaceutical solutions established by international regulatory agencies. Only neutral solutions can be safely used for inhalation purposes, which is reflected by a pH value in the range of 6.5 to 7.5 (at 25 ºC). Acidic pH has been reported to promote bronchoconstriction and cough in nebulized anti-asthmatic solutions [110]. pH is determined by measuring the free hydrogen ions that are in the solution, reported in logarithmic units, and each unit represents a 10-fold change in the acidity/basicity of the solution.

. The solution is acidic if there are many free hydrogen ions, exhibiting a low pH, and basic when the quantity of hydrogen ions is low, reflected by a high pH [111].

1.6.5 Encapsulation Efficiency for RNA

Encapsulation Efficiency (EE) aims to calculate the RNA percentage that is enclosed inside the LNPs. This is an important quality attribute since RNA that is not encapsulated will degrade during the path until the target cell due to RNases present in the body. Fluorescence-based quantification is a widely used method for EE determination in RNA LNPs [112]. The method measures the fluorescence intensity of RNA binding with a fluorescent dye, RiboGreen reagent, that without RNA binding is neglectable. Since the dye cannot enter inside de LNP it cannot bind with the RNA encapsulated inside the LNP core, enabling the quantitation of solely unencapsulated RNA and total RNA present in solution when its promoted LNPs lyse [113].

The encapsulation efficiency is based on the difference between the fluorescence of RNA in the solution after LNPs lysis and the fluorescence of unencapsulated RNA before LNPs lysis. When the solution presents high EE percentages (> 80 %) it can be concluded that LNPs encapsulated almost all RNA added during the production process, and that RNA was not released again with time, which is a sign of good colloidal stability. On the opposite, low EE represents poor colloidal stability.

1.6.6 RNA integrity: gel electrophoresis and HPLC

Even though good EE values mean that encapsulated RNA has not leaked from the LNPs, it does not reflect the ability of the RNA to have the desired effect in the target site. Thus, it is necessary to evaluate the RNA integrity inside the LNPs core.

High-Performance Liquid Chromatography (HPLC) is a reliable method for the separation of large RNA compounds of up to 8000 nucleotides through an ion reverse phase liquid chromatography column [114]. This column works with a hydrophobic nonpolar stationary phase and a mobile polar phase with an ion-pair reagent (usually an alkylated amine). During the process, the amine's alkyl chains bind to the lipophilic stationary phase, leaving the cationic part of the molecule that binds with the negatively charged part of nucleic acids, which promotes hydrophobic separation. Triethylamine (TEA), Dibutylamine (DBA), and Diisopropylethylamine (DIPEA) are some examples of ion-pairing reagents added to the mobile phase [115], [116]. Comparison between RNA standard sample peak size area, shape, and retention time with the sample allows an understanding if RNA is fully operational or if it has degraded.

An orthogonal method to evaluate RNA integrity is gel electrophoresis, which recovers separately nucleic acids based on their charge and dimensions. In this method, an electric current is applied to an agarose gel and, consequently, the samples move through the gel at different velocities. Heavier molecules will remain closer to the beginning of the gel while lighter molecules will travel further and settle at the end of the gel. This is a qualitative method without as much sensibility and resolution as

liquid chromatography since the integrity of the RNA is evaluated by visually comparing if the fluorescent RNA layer that is visible in the standard aliquot is at the same height as the sample [115].

1.6.7 Aerodynamic particle size distribution

The aerodynamic performance of nebulized formulations is a critical quality attribute with high importance for formulation screening, in an early phase of formulations studies, and for final drug product approval since droplets' behavior after nebulization will dictate the pulmonary region where the drug will deposit [100].

For nebulized formulations, this performance is determined with a cascade impactor, and from the several types of cascade impactors in the market, the Next generation Impactor (NGI) launched by MSP corporation in 2000, was the first designed specifically for the pharmaceutical industry. To comply with USP and EP guidelines its necessary to control the airflow passing to the NGI by using a breathing simulator (BRS), as specified in United States Pharmacopeia (USP) <601> [117]. The BRS enables attaining a sinusoidal cycle of inhalation and exhalation, to mimic the breathing pattern of a healthy adult.

The equipment is based on the segregation of droplets produced by the nebulizer through different stages that will separate the droplets by their aerodynamic size. The NGI has seven stages along a horizontal metal plate where the air flows through and between each stage there are cut-off holes, corresponding to the aerodynamic diameter of each stage, which are reducing their sizes gradually with the stages as observed in Figure 4 [118]. After passing stage 7, the remaining particles are collected in a micro-orifice collector (MOC). For nebulizers, the airflow used is 15 L/min which leads to the cut-off diameters present in Table 3 [119]. Due to the lower flow rate used in nebulization experiments in comparison with DPIs, the other available cascade impactors, with a minimum flow of 30 L/min, are not applicable. However, recent studies have explored partial modification of a fast-screening impactor to reduce airflow down to 15 L/min and enable a faster screening, with some early results being comparable to NGI experiments [120].

Since some of the formulation components may be volatile, a major challenge of NGI experiments of solutions for nebulization is droplet evaporation, caused by the impact of the cold droplets onto the warmer steel surfaces. This can reduce droplet size and lead to the incorrect determination of aerodynamic PSD (aPSD). To overcome this effect, the NGI should be cooled down by conducting the experiments inside an NGI cooler at a temperature of 2 - 8 ºC or by cooling down the NGI in advance inside a refrigerator, for at least 90 min.

Table 3 Cut-off diameter for NGI at flow rate 15 L/min

	Stage 1	Stage 2	Stage 3	Stage 4	Stage 5	Stage 6	Stage 7
Cut off diameter at 15 L/min (µm)	14.10	8.61	5.39	3.30	2.08	1.36	0.98

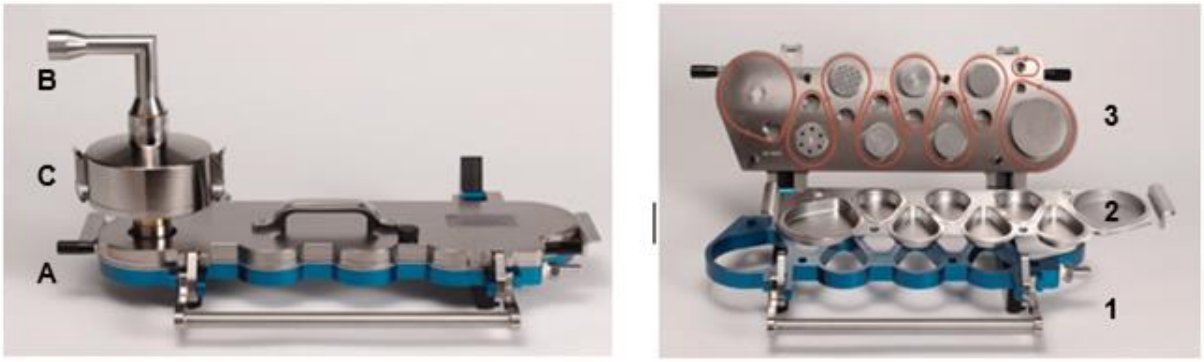

Figure 4 Next generation impactor left: A- 7-Stage apparatus; B- Induction Port; C- Pre-separator (does not apply to nebulizer testing) Right: 1- Bottom frame; 2- Support tray; 3- Lid with interstage

After quantifying the drug deposited at each stage, a log-normal mass distribution of NGI stages is attained and allows to determine the Mass median aerodynamic diameter (MMAD), which is the aerodynamic diameter that represents half of the nebulized drug mass. The MMAD should be lower than 5 µm to facilitate lung deposition in the smaller airways. Additionally, aerodynamic distribution is also reflected by the geometric standard deviation (GSD), calculated according to Equation 3, which measures the variability of the aerodynamic particle sizes [100], [117], [121].

$$GSD = \sqrt{\frac{Aerodynamic\ size\ at\ 15.84\ \%}{Aerodynamic\ size\ at\ 84.13\ \%}}$$

Equation 3 GSD determination based on mass cumulative curve points

The GSD value should be below 2 µm, a value that reflects a monodisperse aerosol particle size [100]. The percentage of particles with an aerodynamic diameter in the inhalable range, between 1 and 5 µm, is expressed by the Fine particle fraction (FPF), determined according to Equation 4 [122].

$$FPF = \frac{Fine\ particle\ dose}{Delivered\ Dose} \times 100$$

Equation 4 Fine particle fraction determination, where Fine Particle Dose (FPD) is the mass of particles with an aerodynamic diameter smaller than 5 μm and the Delivered Dose (DD) is the total mass that is recovered from the NGI (with exception of the drug quantity that remains in the nebulizer).

The MMAD, GSD, and FPF are critical quality attributes of nebulized formulations that reflect the particle deposition in the smaller airways since the deposition site affects drug efficiency.

1.6.8 Delivered Dose of RNA

Delivered dose (DD) is the quantity of solution that potentially reaches the patients' lungs, being a key test to ensure good device/formulation delivery performance. This parameter is measured through the actuation of the device and capturing of the nebulized dose by a filter coupled to a BRS to simulate the inhalation and exhalation pattern of a healthy adult. After a certain period, usually 1 min of nebulization, the filter is collected, and the mass of RNA recovered is used to calculate the delivered dose rate. The filter is replaced by a fresh one and the nebulizer is fully actuated. The totality of the RNA mass captured in both filters corresponds to the total emitted dose [123].

2

MATERIALS AND METHODS

2.1 Materials

The work produced during the thesis can be divided into 3 main parts: 1) LNPs production, 2) LNPs dialysis and nebulization, and 3) analytical characterization. In all these steps it was used the reagents present in Table 4. The composition values (%) of the formulations used in this thesis have been codified due to confidential protection of data.

Table 4 List of reagents used with the respective supplier, purity, and Cas (Chemical Abstracts Service) number. ND: No data

Name	Supplier	Purity (%)	Cas Number
1,2-dioleoyl-3-trimethylammonium propane (DOTAP)	Avanti Polar Lipids, Alabaster	>99	132172-61-3
3 beta-[N-(N',N'-dimethylaminoethane)-carbamoyl]cholesterol (DC-Chol)	Sigma-Aldrich Chemicals, Saint Louis	95	137056-72-5
Cholesterol	Sigma-Aldrich Chemicals, Saint Louis	>99	57-88-5
Distearoylphosphatidylcholine (DSPC)	LIPOID, Ludwigshafen	ND	816-94-4
1,2-dimyristoyl-rac-glycero-3-methoxypolyethylene glycol-2000 (DMG-PEG 2000)	Avanti Polar Lipids, Alabaster	>99	1397695-86-1
Ethanol	AGA, Prior Velho	99.5	64-17-5
Sodium acetate anhydrous	Sigma-Aldrich Chemicals, Saint Louis	>99	127-09-3
Ribonucleic acid transfer, from bovine liver (tRNA)	Sigma-Aldrich Chemicals, Saint Louis	ND	9014-25-9
Water	Milli-Q® Water Purification System	ND	ND
EZ CAP™ EGFP mRNA (5-MOUTP)	APEXBIO, Houston	ND	ND
Phosphate buffered saline (PBS)	Sigma-Aldrich Chemicals, Saint Louis	ND	ND
Poloxamer 188 (P188)	Sigma-Aldrich Chemicals, Saint Louis	ND	9003-11-6
Sucrose	Sigma-Aldrich Chemicals, Saint Louis	>99.5	57-50-1
Sodium Chloride (NaCl)	Merk millipore, Darmstadt	ND	7647-14-5
Arginine	Merk millipore, Darmstadt	ND	74-79-3
Polysorbate 80 (T80)	SEPPIC, Paris	ND	9005-65-6

Triethylamine	PanReac AppliChem, Cinisello Balsamo	99.5	121-44-8
Acetic acid (glacial)	Merk millipore, Darmstadt	100	64-19-7
Acetonitrile	Merk millipore, Darmstadt	100	75-05-8
Agarose	NZYTech, Lisbon	ND	9012-36-6
Tris	NZYTech, Lisbon	>99.9	77-86-1
Ethylenediaminetetraacetic acid (EDTA)	Sigma-Aldrich Chemicals, Saint Louis	99.4	60-00-4
RIBORULER HIGH RANGE RNA LADDER	Thermo Fisher Scientific, Massachusetts	ND	ND
SYBR™ Green II RNA Gel Stain, 10,000X concentrate in DMSO	Thermo Fisher Scientific, Massachusetts	ND	ND
Glycerol, Emsure®, Reag. Ph Eur	Merk millipore, Darmstadt	85	56-81-5
Bromophenol Blue	Bio-Rad, California	ND	115-39-9
SDS Solution 10% (W/V)	Bio-Rad, California	ND	ND

2.2 Methods

2.2.1 LNPs production by Microfluidics

The LNPs production was executed in a set composed of 4 high-pressure syringe pumps dual-NE-1010 from KF technology, Roma (Figure 15A-D), 4 ferrules with integrated filter, 1.6 mm FEP tube, 4 2-way in-line valves, 3 T-Connector, and flangeless ferrules, all from VWR, a staggered herringbone micromixer from Dolomite, Charlestown, and a microscope from dino-lite. The setup was assembled as shown in Figure 5.

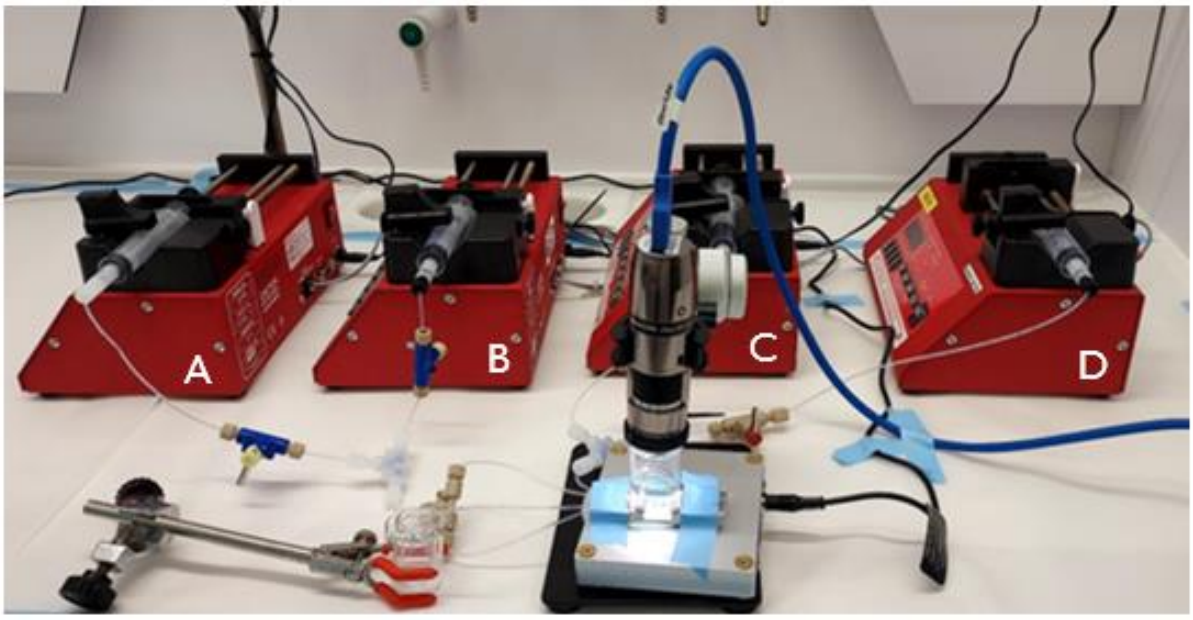

Figure 5 Microfluidics set up for LNPs production

Firstly, the lipid and aqueous phases were prepared separately. For the work developed during the thesis, two different lipid phases were prepared, the first solution was composed of DOTAP, DSPC, Chol, and DMG-PEG 2000, while the second solution was composed of DC-Chol, DSPC, Chol, and DMG-PEG 2000.

Lipids were prepared by measuring their mass individually and then dissolved in ethanol to achieve the desirable ionizable/cationic lipid concentration. This step was performed at 40 ºC to improve dissolution. After completely dissolved, filtration was performed using a 0.2 µm acrodisc filter from Pall coupled to a 10 mL luer lock syringe from VWR, and the solution was stored in a 10 mL luer lock syringe, placed in the syringe pump C (Figure 5) to be used later.

Two aqueous phases were prepared by dissolving the different RNA sodium acetate solution buffer pH 5, prepared with Mili-Q water, sodium acetate, and acetic acid to achieve a desirable concentration of tRNA solution or mRNA solution. The first aqueous phase was prepared with tRNA and buffer, while the second was prepared with mRNA and buffer. The aqueous phase was stored in a 10 mL luer lock syringe placed in syringe pump B (Figure 5) to be used later.

On syringe pump A, it was placed a 10 mL luer lock syringe with sodium acetate solution and, in syringe pump D, a 10 mL luer lock syringe with ethanol for lines purge and cleaning.

Before LNPs production, it was necessary to clean and purge all the lines. Firstly, with the microscope coupled to the micromixer, it was necessary to search for residues that can affect the process. If these residues were present the setup should be disassembled and cleaned.

With no visible residues inside the micromixer, then it was required to pass the lines with sodium acetate buffer (syringe pump A), and then purge the aqueous phase line (syringe pump B) until the first T-connector. After the purge, it was necessary to pass again sodium acetate buffer to avoid LNPs formation when the same process was repeated in the lipid phase (syringe pump C) with ethanol as a buffer (syringe pump D). In the end, it was assessed if there were bubbles inside the micromixer as shown in Figure 6 A.

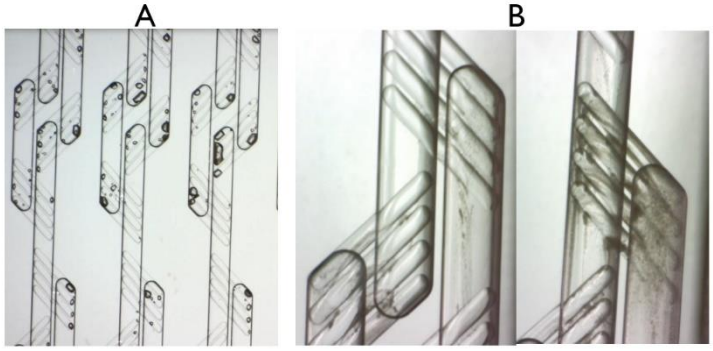

Figure 6 A-Micromixer with air Bubbles; B-Micromixer accumulation after production

With the previous steps evaluated, the LNPs production was started with a defined total flow rate. The first 40 seconds of LNPs production were collected in Eppendorfs since the beginning of production can generate particles with non-homogeneous particle sizes, while the remaining fraction was collected in flasks and used for posterior tests.

The production was stopped when dark spots start to appear in large quantities on the first chaotic mixers as observed in Figure 6 B. The cleaning process was realized by alternating the sodium acetate buffer (syringe pump A) and ethanol buffer (syringe pump D) until no residue was shown in the micromixer. This process should be replicated several times until all lipid and aqueous phases were used.

2.2.2 LNPs dialysis

Dialysis has the objective of replacing the solution where LNPs were produced, ethanol and sodium acetate, with excipients suitable for inhalation. During the thesis, the following formulations were tested: NaCl (A % W/V), NaCl (A % W/V) with Tween 80 (E %W/V), NaCl (A % W/V) with Poloxamer 88 (F %W/V), PBS, PBS with Tween 80 (E %W/V), PBS with Poloxamer 188 (C %W/V), PBS with Poloxamer 188 (D %W/V), PBS with Poloxamer 188 (F %W/V), PBS with Poloxamer 188 (G %W/V), PBS with Poloxamer 188 (H %W/V), PBS with Poloxamer 188 (F %W/V) and Tween 80 (E %W/V), PBS with Sucrose (I %W/V) and Poloxamer (G %W/V), and PBS with Arginine B mM. The dialysis was performed in a slide-a-lyzer mini dialysis device 10K MWCO from Thermo Scientific, Rockford, where 45-50 mL of the formulation were added in the lower part of the cup (Figure 7 B-2) and 2-3 ml of LNPs were added in the upper part of the cup (Figure 7B-1). The cups were stored inside the NGI Cooler from Copley, Therwill, to keep the samples at a temperature between 2 - 8 ºC and with agitation in a mini shaker from VWR to facilitate dialysis as shown in Figure 7 A. The buffer in the lower part of the cup was changed 4/5 times during 2-day dialysis, at every 4-5 hours during the day, and kept with the same buffer during the night.

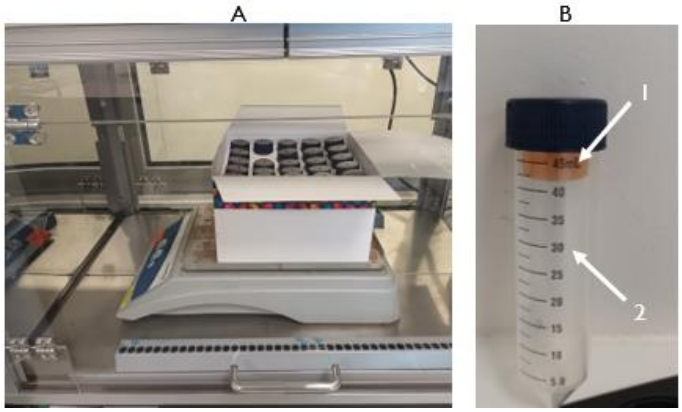

Figure 7 A-Dialysis set up; B- Dialysis cup with 1- dialysis device to place LNPs and 2- falcon to place the desired buffer

2.2.3 Osmolarity

To evaluate the osmolarity, a K-7400 Semi-Micro osmometer from Knauer, Berlin, was used. Before starting measurements, it was necessary to evaluate the status of the equipment with a standard sample, which was ultra-pure water with an osmolarity of 0 mOsm. If the standard measurement was outside the acceptance criteria, equipment calibration with 3 samples of known osmolarity was required. For sample analysis, an Eppendorf from the osmometer was filled with 150 µL and placed in the osmometer for reading. At the end of the reading, after unfreezing the sample, the thermistor and stirring wire was cleaned with deionized water. Osmolarity is evaluated after dialysis, after dilution of the sample, and after nebulization.

2.2.4 LNPs nebulization

Nebulization was performed using an Innospire Go vibrating mesh nebulizer from Philips, and the nebulized sample was collected in a 50 mL falcon attached to the mouth of the nebulizer with parafilm. During nebulization, the nebulizer was placed inside a closed box to avoid inhalation of any aerosolized droplets as shown in Figure 8.

A 2 mL buffer formulation was nebulized three times to compare the nebulization times and understand if the nebulizer was working correctly. Then, 2-6 mL of the sample was nebulized. After the end of nebulization, a 2 mL buffer solution was nebulized to clean the mesh from any remaining LNPs followed by cleaning with deionized water.

Figure 8 Nebulization set up, inside a closed box to contain the release of droplets to the surrounding environment, due to HSE concerns.

2.2.5 Particle size and zeta potential

The particle size, its distribution, and polydispersity index were determined by dynamic light scattering and zeta potential was evaluated by electrophoretic mobility. Both measurements were performed in a Zetasizer Nano ZS from Malvern Instruments.

The particle size and polydispersion index of the samples were measured at 25 ºC with NIBS (Non-Invasive Back Scatter) and an angle of 173º. The samples were prepared in a 1 mL disposable cell with a ratio of milli-Q water/sample of 980:20 for non-diluted samples and 960:40 for diluted samples.

The zeta potential was determined using electrophoretic mobility in a folded capillary cell from Malvern at 25 ºC. The volume of the sample was 600 µL, from which 200 µL were sampled and the remaining 400 µL were composed of milli-Q water.

All measurements of particle size and zeta potential were performed with a stabilization time of 120 s before measurement and a triplicate with 10-20 runs per measurement. After the measurements, the Malvern DTS v5.2 software was used for data acquisition and analysis.

2.2.6 Encapsulation Efficiency

The encapsulation efficiency (EE) was evaluated by a RiboGreen assay which evaluates the fluorescence in a Synergy HTX microplate from Bio Tek reader at 25 ºC and with a wavelength of emission λem = 520 nm and a wavelength of excitation λex = 480 nm [124].

The samples were prepared in a 1 mL Eppendorf, and two types of 800 µL samples were prepared, lysed LNPs samples and non-lysed LNPs samples. For lysed LNPs samples, it was added 200 µL of 2 % (v/v) TE-Triton Buffer to achieve a 1 µg/mL tRNA concentration in Eppendorf and diluted to volume 400 µL with 1X TE-buffer. The non-lysed LNPs were prepared by adding the necessary volume to achieve a 1 µg/mL tRNA concentration in Eppendorf and diluted to volume 400 µL with 1X TE buffer. Both types of samples were incubated at 37 ºC for 10 min, and after cooling to room temperature, 400 µL of diluted RiboGreen was added to each Eppendorf. 200 µL of each sample were placed into a 96-plate well black fluorescent plate from VWR, for posterior reading on the microplate.

An RNA calibration curve was prepared with the same method as the lysed LNPs at different RNA concentrations.

After measuring the plate's fluorescence, the encapsulation efficiency was calculated using Equation 5 [73], where the total RNA is relative to the lysed LNPs and the unencapsulated RNA to the non-lysed LNPs.

$$EE(\%) = \frac{Total\ RNA - Unencapsulated\ RNA}{Total\ RNA} \times 100$$

Equation 5 Encapsulation Efficiency of Lipid Nanoparticles

2.2.7 Aerodynamic particle size distribution

The aerodynamic performance of nebulized droplets was determined with a new generation impactor (NGI). The NGI was placed for at least 30 min inside the NGI cooler to cool down to 2 - 8 ºC. This NGI was coupled to the breathing simulator BRS, a vacuum pump, and a source of compressed air via an induction port connected to an air inlet mixer. All the equipments were purchased from Copley, Therwill.

The vacuum and compressed air flow rates were set at 15 L/min, to provide an average flow rate of 0 L/min when the BRS is stopped. The flow rate was measured with a Copley DFM 2000 Digital flow meter. Then the Copley BRS software was programmed to deliver a volume of 500 mL, which is the tidal volume in a healthy adult, in a sinusoidal breathing pattern with a 2 second inhalation and 2 second exhalation cycle (inhalation/exhalation = 1:1).

The nebulizer was filled with 6 mL of LNPs solution and attached to the mouthpiece adapter. 6 mL was used to increase the detection of the active drug while remaining within the nebulizer's acceptable range of volume (2 – 8 mL). Due to HSE concerns, a plastic bag with holes to enable circulation of flow was placed around the nebulizer to avoid nebulized particles to be inhaled by the analyst (Figure 9).

With all the setup ready, the BRS valve was opened, and the nebulization started immediately after the BRS was initiated. During nebulization, the temperature and humidity inside the NGI cooler were recorded for informative purposes, as well as the total time of nebulization. At the end of nebulization, the flow rate was re-evaluated to guarantee it remained close to 0 L/min when the BRS is stopped.

The NGI was then disassembled and the stages, the inlet mixer, Induction Port (IP) (throat), mouthpiece adapter, interstage, and device were rinsed with 2.5 mL buffer solution to recover the LNPs present in each stage. The stages were placed in agitation for 10 min in the gentle rocker from Copley, the IP in the Sample Preparation Unit 200i from Copley, Therwill, for 10 min at 50 rpm,

while the mouthpiece and the device could not be agitated, thus were maintained in contact with the buffer solution with no agitation for 10 min. The recovery from the interstage was done with a wet swab (with buffer) that is passed in all the NGI inner surfaces. After recovery, the swab was placed inside a falcon tube and agitated in a DUSA Shaker from Copley for 10 min.

The samples were then evaluated using the EE method, where fluorescence was converted in concentration and then in the mass of LNPs. The values of mass at every stage were plotted and a distribution curve was generated by the Copley software CITDAS, from which the results of fine particle fraction, Mass Median Aerodynamic diameter (MMAD), and Geometric Standard Deviation (GSD) can be automatically retrieved.

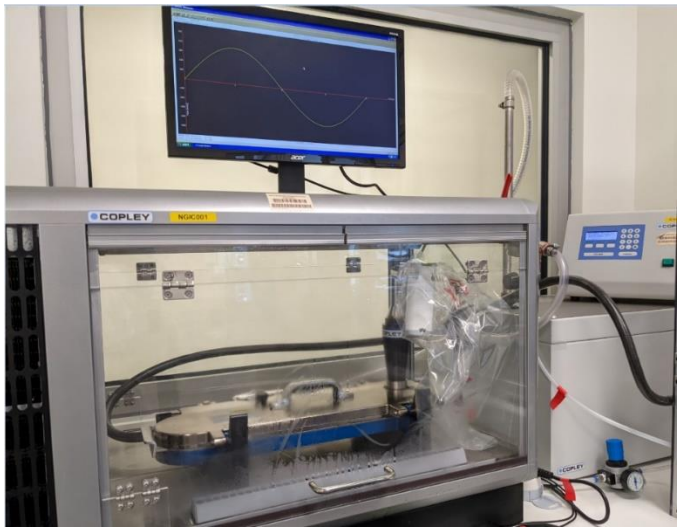

Figure 9 NGI set up for nebulized solutions inside an NGI cooler and a plastic bag for containment.

2.2.8 Delivered dose

For delivered dose evaluation, a similar methodology to the aPSD was performed, where filter support was coupled to the breathing simulator BRS, a vacuum pump, and a source of compressed air via an induction port connected to an air inlet mixer. The vacuum and compressed air flow rates and Copley software were programmed with the same values used in subchapter 2.2.7.

The nebulizer was filled with 2 mL of LNPs solution and attached to the mouthpiece adapter. Due to HSE concerns, a plastic bag with holes to enable circulation of flow was placed around the nebulizer to avoid nebulized particles to be inhaled by the analyst.

With all the setup ready (Figure 9), the BRS valve was opened, and the nebulization started immediately after the BRS was initiated. At the end of nebulization, the flow rate was evaluated again to guarantee it remains close to 0 L/min when the BRS was stopped. Afterward, the filter was removed

from the filter holder and inserted into a falcon, to which 2.5 mL of buffer solution was added. The falcon tube was agitated in a Dusa Shaker from Copley for 10 min.

At the end of the agitation, the filter was compressed, and the solution was collected into a flask. The samples were then evaluated using the EE method, where fluorescence is converted in concentration and then in the mass of LNPs.

Figure 10 Delivered Dose set up for nebulized solutions using a jet nebulizer inside a plastic bag due to health, safety, and Environment (HSE) concerns [123].

2.2.9 RNA integrity

RNA integrity was evaluated by reverse phase ion pair chromatography and gel electrophoresis.

2.2.9.1 Agarose Gel electrophoresis

In the gel electrophoresis method, mRNA was extracted from LNPs with SDS 1 % w/v. From the previous preparation, 16 µL were taken and added to 4 µL of sample buffer (50 mM Tris-HCL, 5 mM EDTA, 25 % glycerol, 0.2 % bromophenol blue, and Syber Green II 5Xare) to denature the sample by heating for 5 min at 70 ºC.

The gel used was a 1 W/W % Agarose gel with TAE 1X as running buffer prepared from a TAE 50X (2 M Tris, 1 M glacial acetic acid, 50 mM EDTA) diluted with autoclaved water. In each

agarose, well 10 µl sample were loaded and as control, an RNA Ladder, RiboRuler High Range RNA Ladder from Thermo Scientific™ was used.

The gel was run at 50 V for approximately 1 h 30 min in Wide Mini-Sub Cell GT from Bio-Rad, California. When the run was finished, the gel was imaged on a Chemidoc MP imaging system from BioRad, California.

2.2.9.2 Ion pair reverse phase chromatography

To assess the mRNA integrity by chromatography, a DNAPac RP column (ion pair reverse phase) with 4-µm particles and dimensions of 2.1 × 100 mm from Thermo Fisher Scientific was used at a flow rate of 0.35 mL/min and temperature of 60 °C. Two mobile phases were prepared, mobile phase A consisted of 0.1 M Triethylamine Acetate (TEAA) buffer and mobile phase B consisted of 50:50 %v/v acetonitrile (ACN) and 0.1 M TEAA buffer.

mRNA was extracted from LNPs using SDS 1 % w/v and targeting a final mRNA concentration of 0.0045 µg/µL. Injections of 20 µL sample with 0.09 µg of mRNA were made. The autosampler was kept at 4 °C to minimize degradation and mRNA was detected by UV at 260 nm.

The chromatography method consisted of an initial 2-min hold at 90 % mobile phase A and 4 % mobile phase B, followed by A linear gradient from 10 to 20 % of mobile phase B in 13 min was done followed by another gradient of mobile phase B from 20 to 90% in 5 min, with a 2-min hold after. It was performed a return to the initial conditions of 90 % mobile phase A and 4 % mobile phase B in 0.1-min and hold for 7.9-min, followed by a 3-min gradient from 0 to 100 % of ACN and hold for 5 min. At 38.10 min, the mobile phase mixture was set to 90 % mobile phase A and 4 % mobile phase B in 0.1-min and hold for 6.9 min.

At the end of the run, the chromatograms were collected and the areas under the peaks were integrated using Empower Version 2.0, Milford.

2.2.10 LNPs stability test

tRNA LNPs stability was evaluated during 100 days at room temperature, in the fridge at 2 - 8 ºC, and frozen at -20 ºC. In frozen samples, it was also evaluated the freeze and thaw cycles by unfreezing a sample flask at a stabilization temperature of 2 - 8 ºC every time it was necessary to perform sample readings. At the end of the measurement, the flask was frozen again. To evaluate the stability of nanoparticles, it was measured the particle size and encapsulation efficiency on the specified time points according to methods described in subchapters 2.2.5 and 2.2.6.

3
RESULTS AND DISCUSSION

The creation of a nebulization platform for RNA LNPs requires in the initial phase, explore the LNPs production process, understand its potential critical parameters, and perform a formulation screening without incurring into high costs. For that reason, the RNA molecule used for the first tests was tRNA, which was a low-cost RNA molecule available at Hovione, that performed as a model molecule for assessing LNPs integrity and colloidal stability.

3.1 tRNA LNPs production: troubleshooting, characterization, and stability

The tRNA LNPs production was performed through the microfluidics production method described in subchapter 2.2.1, using a lipid phase composed of DOTAP, DSPC, Chol, and DMG-PEG 2000. The aqueous phase was composed of sodium acetate and tRNA with a certain concentration.

The first step in the production process was a micromixer inspection since it was noticed that filament accumulation inside chaotic mixers could occur (Figure 11). This evaluation was extremely important since this accumulation of material could affect the chaotic mixers flow, causing a negative impact on the LNPs production.

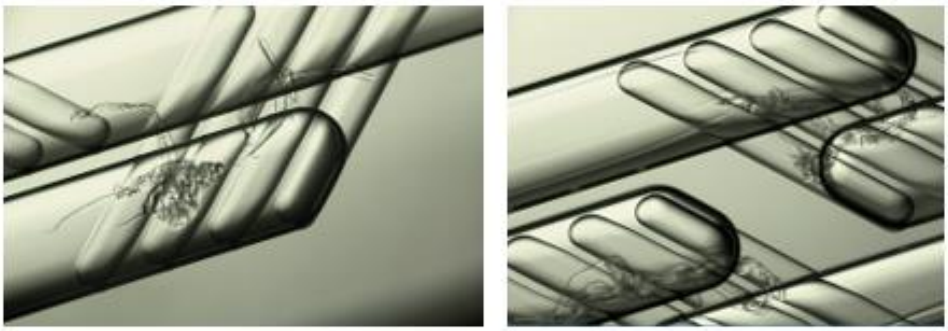

Figure 11 Microscope images of accumulated material (filaments) inside the micromixer

When filaments were seen inside the chaotic mixers, different cleaning reagents from an approved list provided by the manufacturer [125], were used in the micromixer to promote unclogging. To overcome this challenge, new strategies were implemented in the system to reduce the probability of filaments accumulation, namely: ferrules with filters were placed in all lines to avoid filaments passage, the lipid phase was filtered before production, and a portable microscope was placed above the micromixer for continuous monitorization of LNPs production and early filament detection.

With the probability of clogging the micromixer minimized, several LNP productions were performed. Occasionally, it was noticed that after a few minutes of production, dark spots were observed in the micromixer (Figure 6 B), and the LNPs collection needed to be stopped. These dark spots may happen due to a gradient between the two phases in certain parts of the chaotic mixer, which can lead to the accumulation of material.

All tRNA LNPs batches were characterized for particle size and PDI, which is a fast characterization test to determine if LNPs presented a homogeneous particle size after production (as defined in subchapter 1.6.1 particle size should be < 200 nm and PDI < 0.300). It was possible to observe in Graph 1 that the 19 tRNA LNPs batches presented a similar particle size and PDI leading to an average value of 48.88 ± 3.73 nm for particle size and an average value of 0.198 ± 0.032 for PDI. The presented results show that the microfluidic LNPs production process is reproducible. The batches 12 to 14, 21, and 23 were not present in the graph because they correspond to batches with different compositions than previous ones.

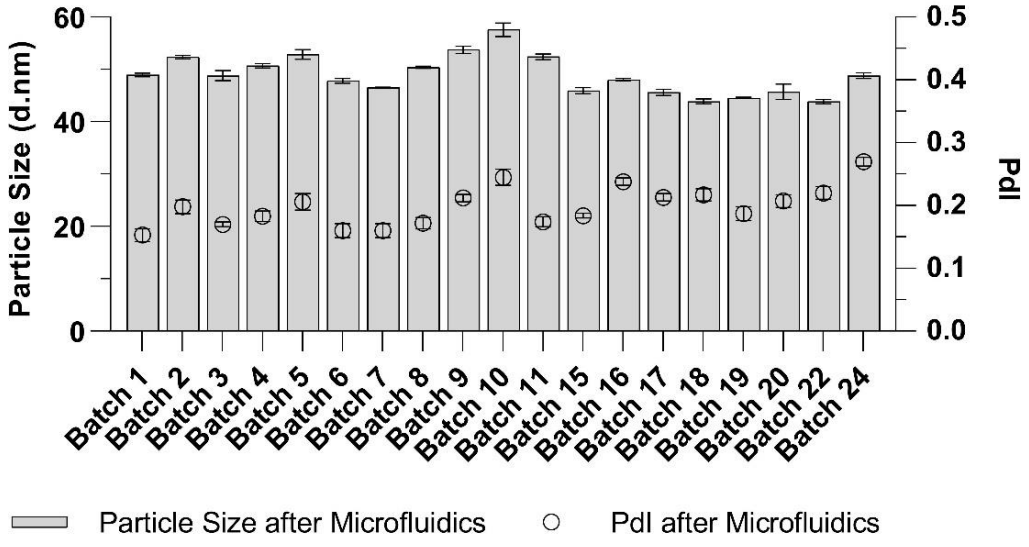

Graph 1 Compilation of all batches of LNPs plotted against their particle size and PDI

Although there was no available literature about LNPs encapsulating tRNA, the particle size and PDI observed were in accordance with what was expected of LNPs that have as payload nucleic acids [126]. Patisiran reported SiRNA encapsulation in LNPs (RNA molecule with a similar size to tRNA) with similar particle size values [127].

With produced tRNA LNPs achieving the particle size quality attributes, it was necessary to evaluate the storage conditions that would provide longer colloidal stability. In the literature, it was reported that LNPs stability can be affected physically or chemically. Chemical destabilization can occur due to the degradation of lipids present in LNPs that are prone to oxidation or hydrolysis. Physical destabilization can occur due to aggregation, fusion, or leakage of encapsulated material during production or storage time [53].

Thus, colloidal stability of tRNA-LNPs suspended in ethanol and sodium acetate was studied at room temperature (20-25 ºC), at 2−8 ºC, at -20 ºC and freeze/thaw cycles, through particle size, PDI, and encapsulation efficiency evaluation for 100 days.

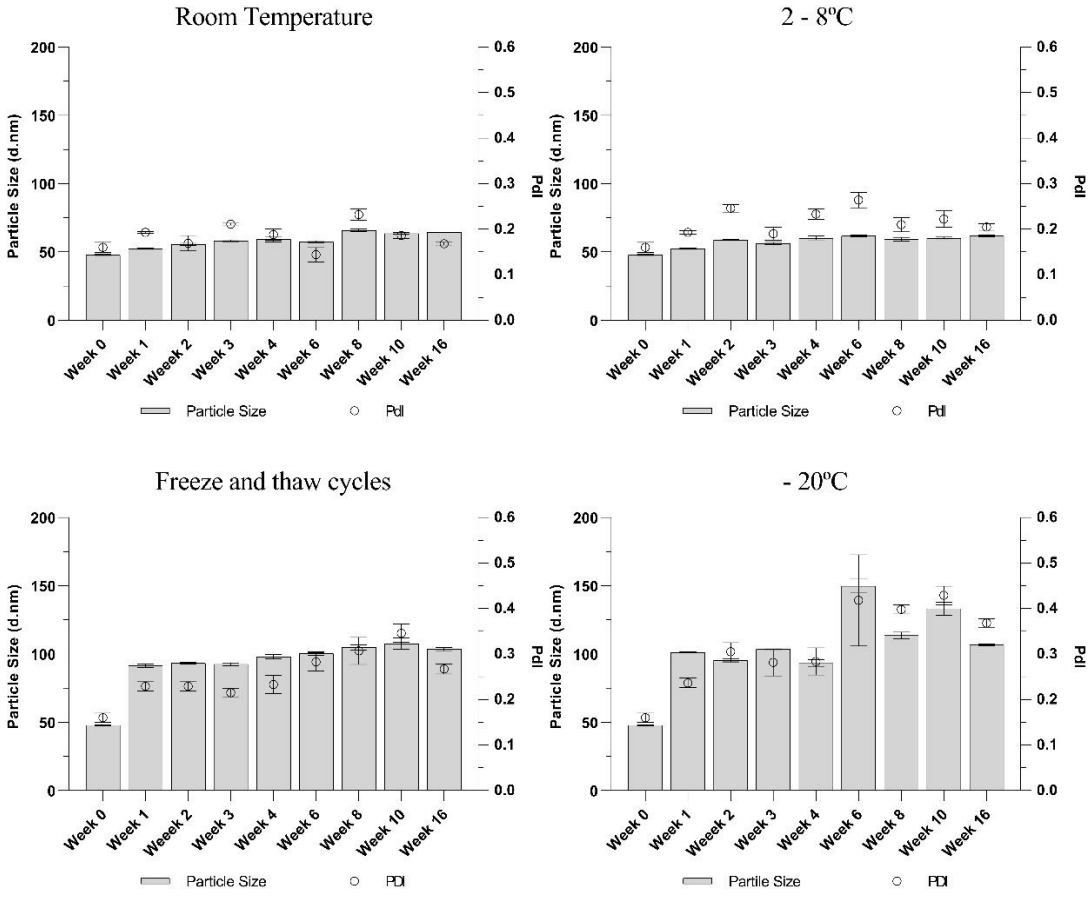

Graph 2 tRNA LNP's particle size and PDI stability test for storage at room temperature (20-25 ºC), at 2-8 ºC, at -20 ºC, and freeze and thaw cycles.

Samples stored at room temperature and at 2-8 ºC did not present any relevant increase in particle size or PDI during the 16-week stability test period. The results obtained were similar to other stability tests realized by other authors, for example, a study where stability tests with LNPs with similar composition, but encapsulating SiRNA and dialyzed in PBS buffer were performed, presented constant particle size and PDI over 18 months when stored at 4 ºC [128]. In a different study, it was shown that diluting LNPs in PBS and storing at pH 7.4 at 2-8ºC can preserve LNPs characteristics for up to 160 days [129].

After the first week of freeze/thaw cycles, LNPs almost doubled their particle size but remained within acceptable quality attributes until week 4. After that period of time the PDI was outside the acceptable range (particle size < 200 nm and PDI < 0.300). The particle size increase is related to the freezing process since when LNPs solution freezes, it occurs the formation of an ice phase and, consequently, an LNPs concentrated solution phase which leads to irreversible fusion and aggregation [128] – [131].

Frozen samples presented a PDI close to the acceptable limit from week 1, with small variations in particle size until week 4, and after that time the PDI increased to values out of the acceptable range, which means that LNPs lost their colloidal stability. The variations presented until week 4 could be related to the fact that each sample was frozen in an Eppendorf with a small volume, which could lead to heterogeneous environments and different frozen behaviors, manifesting itself in differences in particle size after freezing.

The encapsulation efficiency of LNPs was only evaluated at the beginning and end of the stability test as observed in Table 5 since EE uses expensive reagents. All the results at the beginning and end of the stability test did not present significant changes in EE, which was expected for samples at room temperature and at 2 - 8 ºC due to its homogeneous results in particle size tests. The EE results of frozen samples and from freeze/thaw cycles showed that particle size increase was not related to LNPs leakage, but to fusion or aggregation of LNPs when frozen since EE did not present changes after 100 days.

The stability test results allowed to conclude that all LNPs should be stored at 2-8 ºC and that these storage conditions will preserve LNPs characteristics for up to 16 weeks.

Table 5 Encapsulation efficiency results on day 3 and day 100 of the stability test

Sample	Encapsulation Efficiency (t = 3 days) (%)	Encapsulation Efficiency (t = 100 days) (%)
Room Temperature	98	97
2-8 ºC	99	99
-20 ºC	99	99
Freeze/thaw cycles	98	98

3.2 tRNA LNPs screening formulations for nebulization

The solution where the LNPs were produced was not suitable for human inhalation, since it contained high ethanol quantities that can cause throat irritation, coughing, and choking. For that reason, the different tRNA-LNPs batches produced were dialyzed into different formulations. It was performed a formulation screening, to assess which formulation would provide better nebulization conditions:

- NaCl A % W/V
- NaCl A % W/V with E % W/V Tween 80
- NaCl A % W/V with F % W/V Poloxamer 88
- PBS
- PBS with E % W/V Tween 80
- PBS with F % W/V Poloxamer 188

The dialysis was performed according to the dialysis method described in subchapter 2.2.2. Considering that, 2 mL of every dialyzed formulation were nebulized according to the nebulization method described in subchapter 2.2.4, to evaluate colloidal stability after microfluidics, dialysis, and nebulization, through particle size tests as observed in Graph 3.

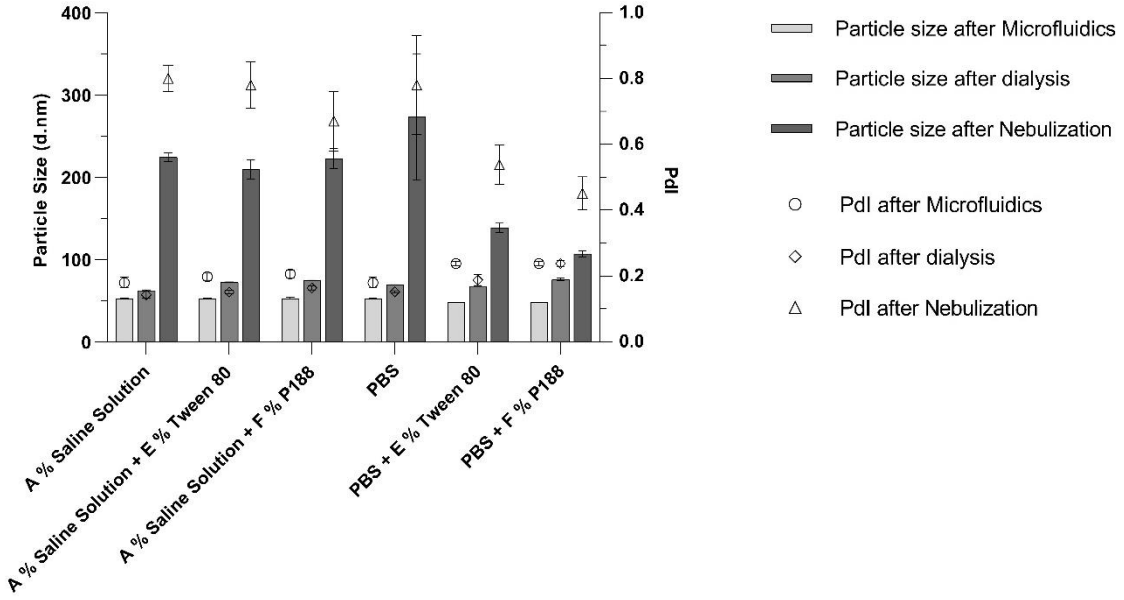

Graph 3 Particle size and PDI comparison of different formulations after microfluidics, after dialysis, and after nebulization

It was observed that after the dialysis step, the particle size had a small increase and at the same time the PDI decreased, as reported in another study [133]. The referred literature does not explain this effect [134], however since these were small changes in size (< 20 nm), one possible explanation for that increase could be the small differences between the formulations, which could lead to the particles moving slightly slower, which in turn could be perceived as a larger size. Nevertheless, both parameters were within quality attributes (Particle size < 200 nm and PDI < 0.300).

All formulation results after nebulization showed that the mechanical stress caused by the LNPs passage through the vibrating mesh destabilizes LNPs, resulting in particle size and PDI increase. We hypothesize that, in a non-optimal formulation, the particle size and PDI increase are the results of the vibrating nebulization process, which may promote either aggregation, fusion, and/or disintegration of LNPs.

Formulation screening was started from the simplest formulation and, according to the results obtained after nebulization, other excipients were added to achieve LNPs colloidal stability. In the first screening formulation, the main objective was to understand which excipient, NaCl A % or PBS, provided better colloidal stability to LNPs by reducing the impact of the nebulization's mechanical stress.

The formulation with only NaCl A % presented a smaller particle size than the formulation with only PBS after nebulization, but when other excipients were added to the buffer formulations, the results from formulations based on PBS presented better PDI and particle size than NaCl A % based

formulations. These results allowed to conclude that PBS based formulations with other excipients offered better colloidal stability than NaCl A % based formulations with excipients. Despite this tendency, all experiments had a poor nebulization performance with a PDI and a particle size higher than the acceptable quality attributes.

The two formulations with the best performance, PBS with E % T80 and PBS with F % P188, were analyzed in detail to understand how particles were affected by nebulization. Intensity graphs provided by Malvern software make possible to evaluate the particle size through different intensity peaks which correspond to a determined particle size.

Graph 4 shows that, after dialysis, there was a homogeneous particle size distribution with only one peak. Even though this peak remained in the same position after nebulization, a second peak with a larger size appeared. This leads to the conclusion that, after nebulization, part of the LNPs can hold the mechanical stress caused by the vibrating mesh while another part of the LNPs may merge or aggregate which originates a peak with larger dimensions.

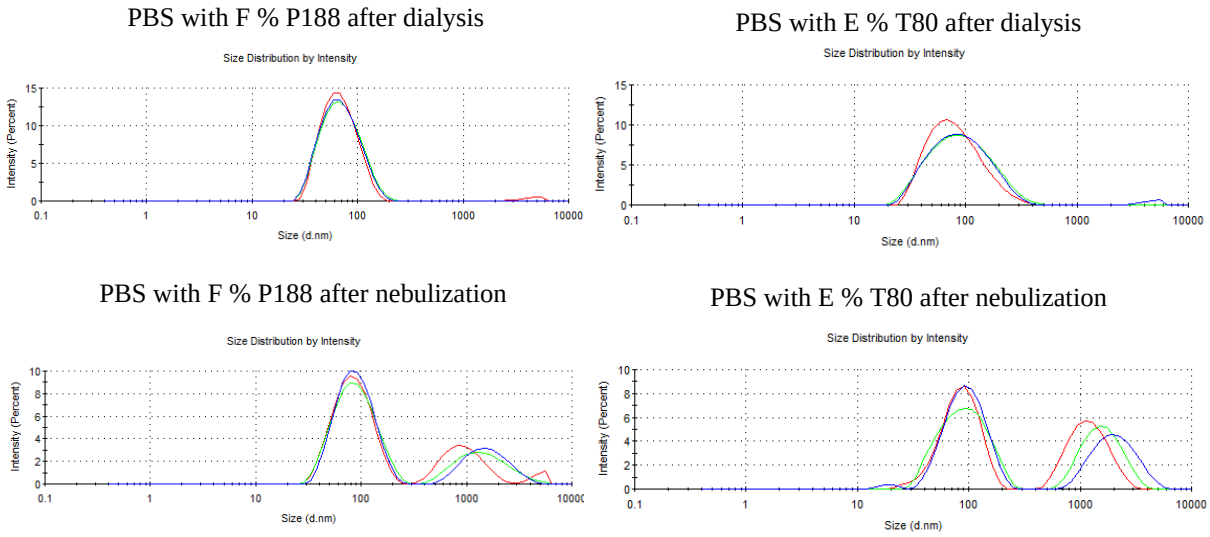

Graph 4 Intensity particle size graphs from Malvern DTS v5.2 software after dialysis and after nebulization (n=3)

It was concluded that for further tests PBS based formulations should be used since PBS presented better results than NaCl A % based formulations. Also, different excipients with PBS should be evaluated since none of the previous formulations presented colloidal stability after nebulization.

Considering the previous results, the following screening formulations based on PBS plus additional excipients were tested to evaluate the colloidal stability of LNPs:

- PBS with Poloxamer 188 (F % W/V) and Tween 80 (E % W/V)
- PBS with Sucrose (I % W/V) and Poloxamer (G % W/V)
- PBS with Arginine B mM.

Particle size characterization tests were performed after production, dialysis, and nebulization and compared with the two best performing formulations from previous results, to evaluate possible improvements in colloidal stability

Graph 5 showed that particle size results after nebulization in comparison with the best performing formulation have higher values for particle size and PDI. As observed previously, after nebulization the formulations presented two populations of distinct sizes in intensity graphs. None of the formulations evaluated provided enough colloidal stability to LNPs to support the mechanical stress of the vibrating mesh nebulizer (particle size < 200 nm and PDI < 0.3).

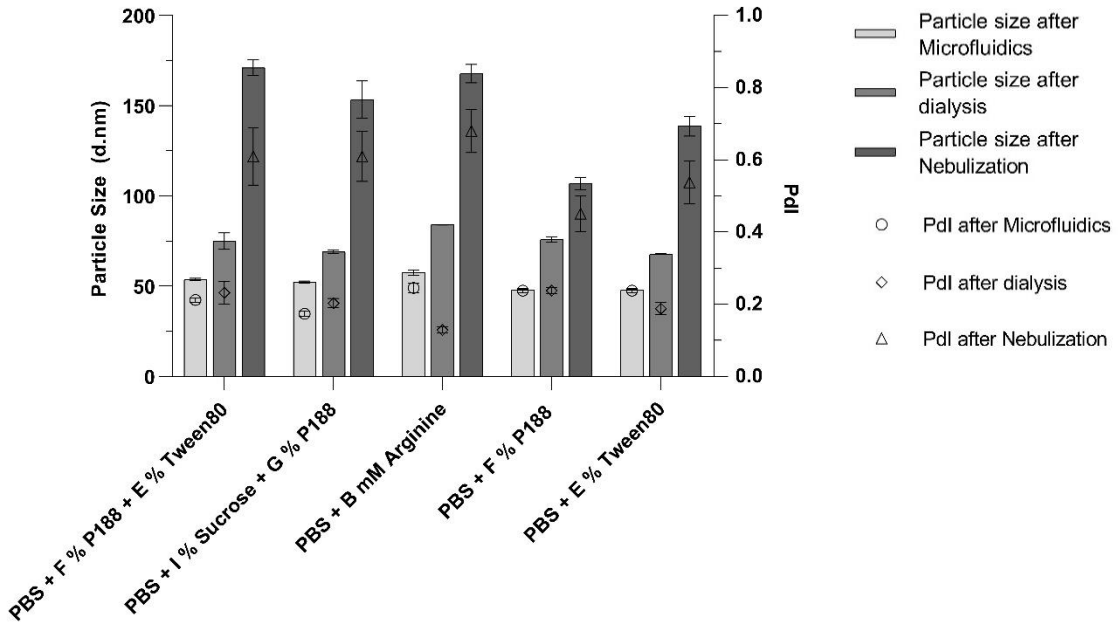

Graph 5 Particle Size and PDI of different formulations with PBS buffer after microfluidics LNPs production, after dialysis, and after nebulization, and comparison with two best formulations from Graph 3

Since none of the screening formulations was producing acceptable results for inhalation, it was evaluated the possibility of optimizing excipients concentration in the formulation which presented better stability. For that reason, PBS with P188 was tested with different concentrations of P188 (W/V): C %, D %, F %, G %, and H % to understand if increasing or decreasing the P188 concentration affected particle size and PDI as observed in Graph 6.

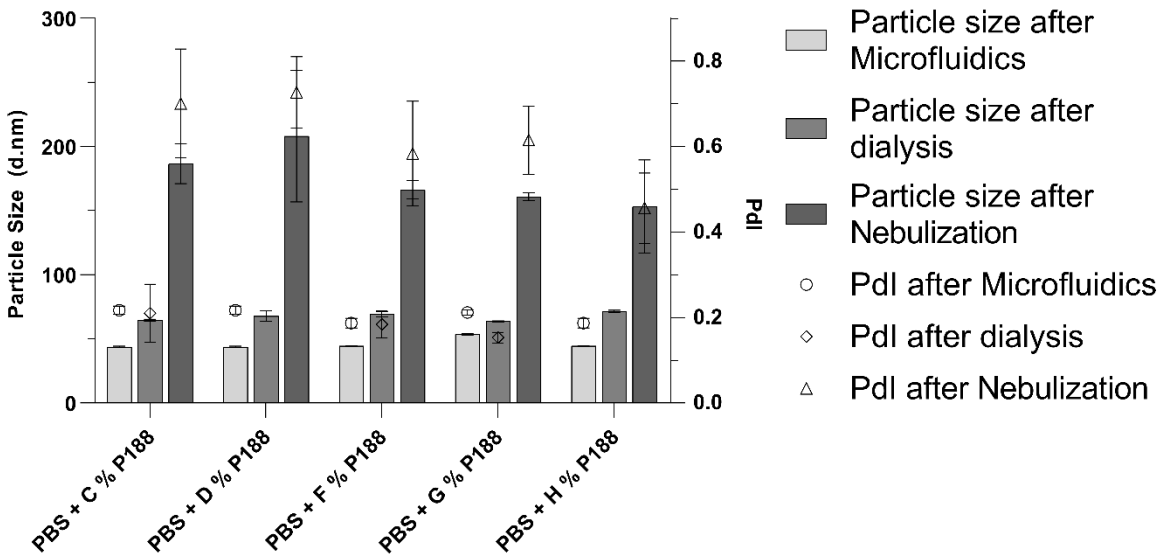

Graph 6 Particle size and PDI comparison of screening formulation of PBS with different P188 concentrations after microfluidics, after dialysis, and after nebulization

In comparison with the previous P188 concentrations tested, F % P188, formulations with lower concentrations of P188 presented higher PDI and particle size after nebulization, while formulations with a higher concentration of P188 presented lower particle size. PBS with H % P188 was the formulation with lower PDI, however, the PDI continued to stay outside the acceptable range, which led to the conclusion that P188 concentration should also remain at the lowest feasible concentration since high concentrations can promote toxic effects.

Since formulations with a high concentration of P188 did not have a significant improvement in colloidal stability in comparison with PBS with F % P188, it was concluded that the optimal P188 concentration should be maintained at F %, although other formulations should be tested since none of the screening formulations supported the mechanical stress promoted by nebulization.

3.3 Osmolarity's importance in LNPs nebulization

As referred in subchapter 1.6.3, osmolarity is a critical quality attribute for pharmaceutical solutions and its value should remain between 300 - 310 mOsm.

Osmolarity was tested for the two best performing formulations after dialysis, which showed values two times higher than the target, as presented in Table 6. To adjust the solution's osmolarity, a dilution curve was performed to understand the dilution ratio necessary to achieve the intended osmolarity values, observed in Graph 7.

Table 6 Osmolarity of two formulations after dialysis

Sample	Osmolarity (mOsm)
PBS with F % P188	601
PBS with E % T80	620

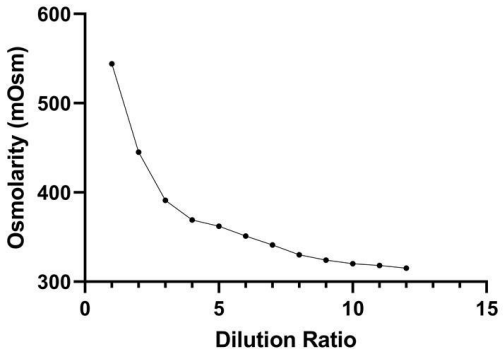

Graph 7 Osmolarity dilution curve with LNPs in formulation with PBS

It was concluded that to achieve an osmolarity close to 300 mOsm for formulations with PBS, it was necessary to perform a dilution of 1:10 V/V, which was the ratio adopted for posterior screening formulation developments.

3.4 Nebulization of tRNA LNPs diluted formulations

Since the two best formulations (PBS with E % T80 and PBS with F % P188) presented particle size and PDI close to acceptable quality attribute values (particle size < 200 nm and PDI < 0.300), it was studied the colloidal stability behavior of tRNA LNPs when those formulations were diluted in a ratio of 1:10 V/V, into the solution containing the respective excipients, either PBS with E % T80 or PBS with F % P188, to reach the correct osmolarity. Formulations were characterized for particle size, encapsulation efficiency, and osmolarity tests.

The particle size results in Graph 8 showed that, for both formulations, there was an increase in particle size after dialysis, changing from 62.22 ± 0.32 nm to 78.85 ± 0.81 nm for PBS with F % P188 formulation and from 59.98 ± 0.54 nm to 86.38 ± 0.92 nm for PBS with E % T80 formulation, while PDI had a decrease in both formulations as reported in previous non-diluted formulation screening.

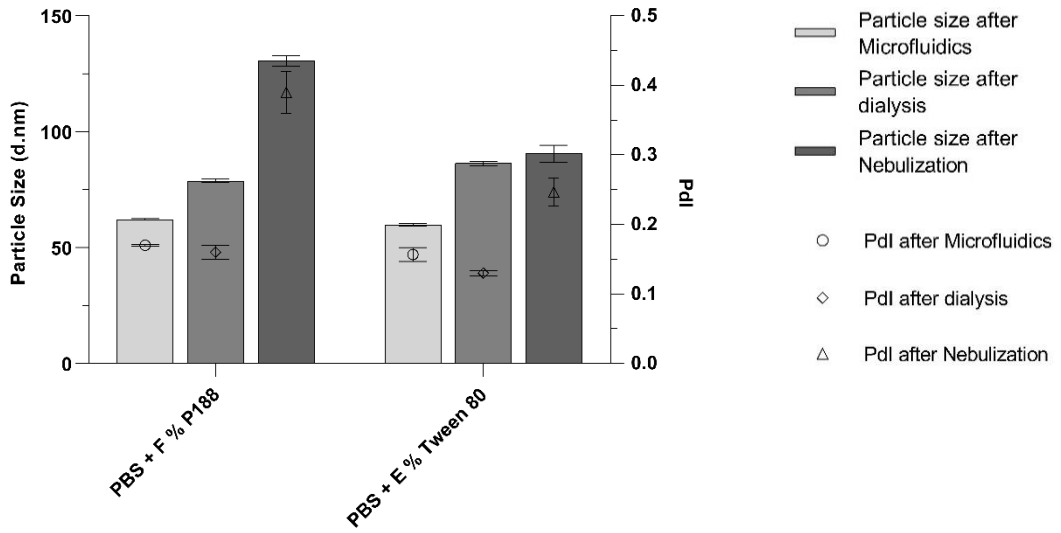

Graph 8 Particle size and PDI of diluted screening formulations after microfluidics, after dialysis with a dilution ratio of 1:10 (V/V), and after nebulization (n=3)

The osmolarity reported in Table 7 allowed to conclude that the dilution ratio achieved the correct osmolarity values (300-310 mOsm), and nebulization did not affect the osmolarity, which was aligned with the expectations, since during the nebulization process no concentration or excipient change was promoted.

Table 7 Osmolarity of formulation PBS with E % T80 and formulation on PBS with F % P188, after production, after dialysis and dilution, after nebulization

Sample	Osmolarity After dialysis (mOsm)	Osmolarity After dilution (mOsm)	Osmolarity After Nebulization (mOsm)
LNPs with PBS and E %T80	620	309	307
LNPs with PBS and F %P188	601	307	301

After nebulization, the formulation PBS with F % P188 showed an increase of the particle size to 130.5 ± 2.25 nm with a PDI of 0.390 ± 0.030. Although the size of the nanoparticles was still within an acceptable range, the PDI value above 0.3 was not acceptable. In Graph 9, this formulation presented two different size LNPs peaks generated during nebulization, which indicate LNPs fusion, aggregation, and/or RNA leakage from the LNPs during the process.

With the EE test was possible to exclude the RNA leakage hypothesis since results presented in Table 8 showed that EE after nebulization remained similar to EE after dialysis and dilution. So, it can be concluded that PBS with F % P188 does not support nebulization mechanical stress and promotes fusion or aggregation of particles.

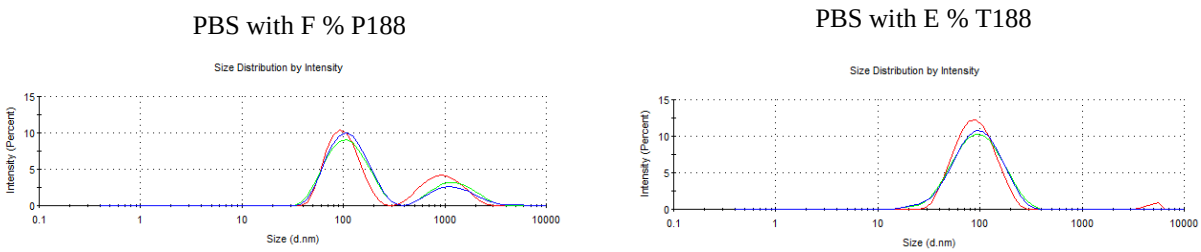

Graph 9 Particle size distribution (intensity) after nebulization in formulations with diluted ratio 1:10 V/V (n=3)

Regarding the formulation with PBS and E % T80 after nebulization, the results showed that the LNPs size did not increase with nebulization, presenting a value of 90.52 ± 3.63 nm with PDI of 0.247 ± 0.02, and EE tests, with values of 99 % after dialysis and 94 % after nebulization, proved that there was no significative tRNA leakage to the solution during all the procedure steps.

Table 8 Encapsulation efficiency of formulation PBS with E % T80 and formulation on PBS with F % P188, after production, after dialysis, dilution, and nebulization

Sample	Encapsulation Efficiency After Production (%)	Encapsulation Efficiency After dialysis and dilution (%)	Encapsulation Efficiency After Nebulization (%)
LNPs with PBS and E % T80	98	99	94
LNPs with PBS and F % P188	99	99	99

The results of tRNA LNPs formulation with PBS and E % T80 complied with the target quality attributes defined above, which are promising results for achieving the first screening formulation that can sustain the mechanical stress induced by the vibrating mesh nebulizer. When compared to P188, T80 showed a greater stabilization and/or protection effect to the stress caused by nebulization, since it complied with all quality attributes defined and no secondary populations of LNPs were registered, indicating that this may be an excipient to be considered when developing formulations for LNPs with nucleic acids. Also, Tween 80 has the advantage that it has been approved for inhalation in the quantity of 1 mg per day.

3.5 Aerodynamic performance of nebulized formulations

Aerodynamic performance is a critical attribute for understanding the efficiency of drug delivery into the lungs. Upon nebulization, droplets will have a determined size when they leave the nebulizer, and this size will indicate if the drug can reach the deep lungs (in case of droplet size in the inhalable range of 1 – 5 µm), will be exhaled (for particles with droplet size lower than 1 µm), or settle in the upper respiratory tract (for particles with droplet size higher than 5 µm).

Both formulations, LNPs with PBS and E % T80 and LNPs with PBS and F % P188, were subjected to an evaluation of aerodynamic performance through the method described in subchapter 2.2.7. The aerodynamic PSD was determined by NGI, where it was calculated the deposition profile observed in Graph 10 from which was possible to determine MMAD, GSD, and FPF detailed in Table 9.

According to the nebulizer's manufacturer specification, the Innospire Go should produce droplets with an MMAD of 3.99 µm and FPF of 64.4 % [134]. However, early nebulization studies were showing a bias in the distribution of the aerosol droplets, with higher MMAD and a smaller FPF, as detailed in Table 9, the values produced were within acceptable criteria defined in subchapter 1.6.7 for both formulations.

Table 9 Values of MMAD, GSD, and FPF of nebulized solutions, determined with Copley CITDAS software.(n=1)

Sample	MMAD (µm)	GSD	FPF (%)
LNPs with PBS and E % T80	4.9	2.5	46
LNPs with PBS and F % P188	4.1	2.2	53

Additionally, the deposition profiles observed in Graph 10 attained for both formulations did not correspond to the expected log normal distribution. The low mass recovered from stage 7 and MOC leads to an apparent larger MMAD.

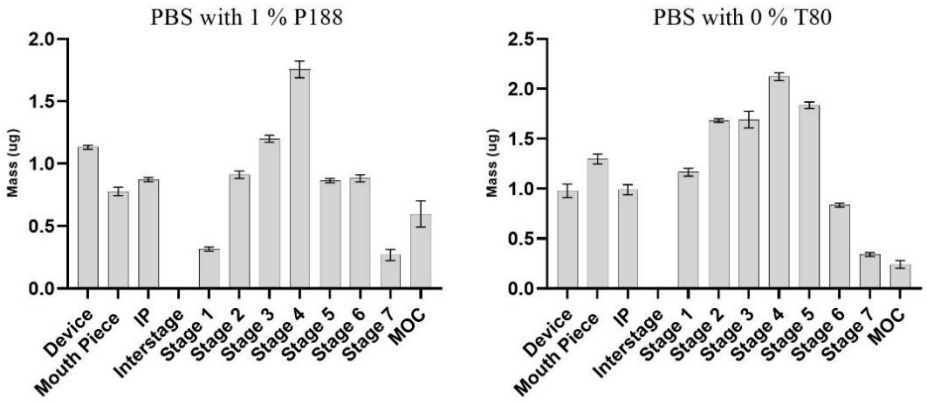

Graph 10 Mass deposition profile of NGI test for formulation PBS with F % P188 and PBS with E % T80 (n=1)

This challenge could be related to the low LNPs concentration in the recovery process since after nebulization, the nebulized solution was further diluted with an additional 5 mL of buffer (inherent to the analytical method process for sample recovery from the NGI apparatus). This leads to concentration values close to the detection limit and results in higher errors associated. To improve the detection, the dilution volume of the samples was decreased from 5 mL to 2.5 mL. Further improvement can be achieved by using more sensitive detection kits available commercially.

Other possible justifications for low mass recovery from stage 7 and MOC were that this suspension formulation was not suitable for this device, or that the cleaning process after nebulization was non-optimum between each nebulization, or that the nebulizer had a malfunction due to excessive use during the screening process. To test those hypotheses, an NGI experiment was performed with a commercial product composed of salbutamol, since the supplier provides target nebulization values for this small molecule.

As observed in Table 10 salbutamol nebulized solution presented a higher MMAD than the reference values, although the value remains in the inhalable range, and lower FPF values than the nebulizer's specification.

Table 10 Comparison between literature values and produced values of MMAD, GSD, and FPF for salbutamol molecule

Sample	MMAD (µm)	GSD	FPF (%)
Salbutamol literature values [134]	3.99	2.1	64.4
Salbutamol nebulizer performance	5.18	2.3	40.8

The results presented in Graph 11 show a low mass recovery from stage 7 and MOC in comparison with what was supposed for a target nebulization. Since the formulations under study had similar results to the reference salbutamol solution, it was decided to proceed with aerodynamic performance studies. However, lower MMAD and FPF were determined for both reference solution and LNPs formulations indicating there might have been alterations to the nebulizer's mesh.

In an attempt to understand the cause of the suspected impacted mesh, microscope photographs were taken. As observed in Figure 12, no visible alterations of the mesh were seen when compared with a reference nebulizer. Even though the cleaning procedure was performed according to the manufacturer's instructions for the nebulization of small molecules, it might need to be optimized for more frequent utilization with innovative products, such as in a research and development setting. Thus, the different mass distribution profiles attained were possibly due to a defective cleaning process or nebulizer malfunction caused by excessive use.

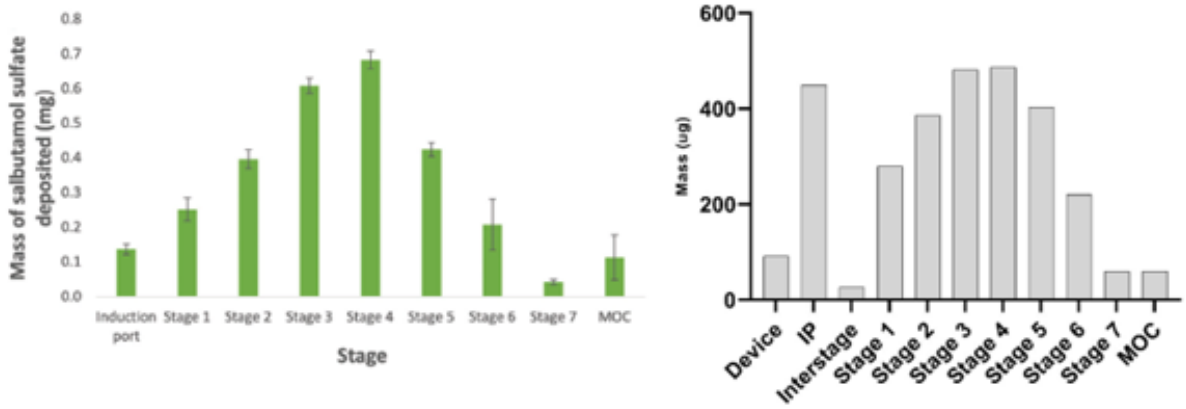

Graph 11 Comparison between the mass deposition profile for a salbutamol solution with a vibrating mesh nebulizer Inno-spire Go according to the literature (left) [120] and determined experimentally (right).

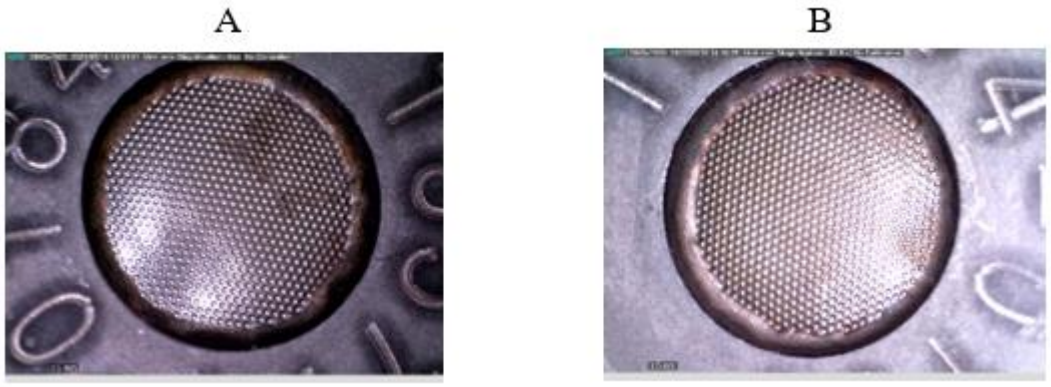

Figure 12 microscope comparison between a reference vibrating mesh nebulizer (A) and the vibrating mesh nebulizer used in the formulation development (B) with a magnification of 64X.

Although the nebulizer's mesh was slightly affected, the aerodynamic particle size distribution for the formulations under study was very similar to that presented by a reference salbutamol solution, indicating the LNP formulations had a good aerodynamic performance throughout nebulization. Despite the results have been biased to larger dimensions, the results will be accepted for comparison purposes and to assess whether excipients significantly impact aPSD.

Since the PBS with E % T80 formulation presented a particle size, osmolarity, encapsulation efficiency, and aerodynamic performance compliant with quality attributes, this was the formulation chosen to perform extensive formulation and aerodynamic performance characterization and to evaluate the reproducibility of the formulation in all process steps (production, dialysis, dilution, and nebulization).

3.6 Characterization of nebulized tRNA-LNPs in PBS E % T80 (1:10) formulation

Characterization of tRNA LNPs with PBS and E % T80 was performed to evaluate the particle morphology, capacity to encapsulate tRNA, and aerodynamic performance from the beginning of production of LNPs up to nebulization. tRNA integrity was not evaluated due to a lack of internal methodologies availability, since the development of a method (chromatography for example) for tRNA integrity evaluation could not fit within the time frame of this thesis work.

Graph 12 shows that LNPs particle size increases after dialysis to 73.63 ± 0.55 nm, with a decrease in PDI, 0.167 ± 0.010, as discussed in subchapter 3.2 (microfluidics results had a particle size of 48.83 ± 0.52 and a PDI of 0.27 ± 0.01). Similar particle size was reported after dilution, 74.54 ± 1.00 nm, whereas PDI increased, 0.186 ± 0.012, although none of the results presented significative

changes that could promote results outside quality attributes (Particle size < 200 nm and PDI < 0.300). The encapsulation efficiency results showed constant EE in all steps, as observed in Table 11.

Particle size and PDI were slightly increased by nebulization since it obtained an average particle size of 79.00 ± 1.87 nm and PDI of 0.238 ± 0.02. In the encapsulation efficiency test, it was observed a decrease from 98 % to 94 %. The decrease in EE accompanied by the PDI value increase could be caused by a small quantity of LNPs lysed during nebulization.

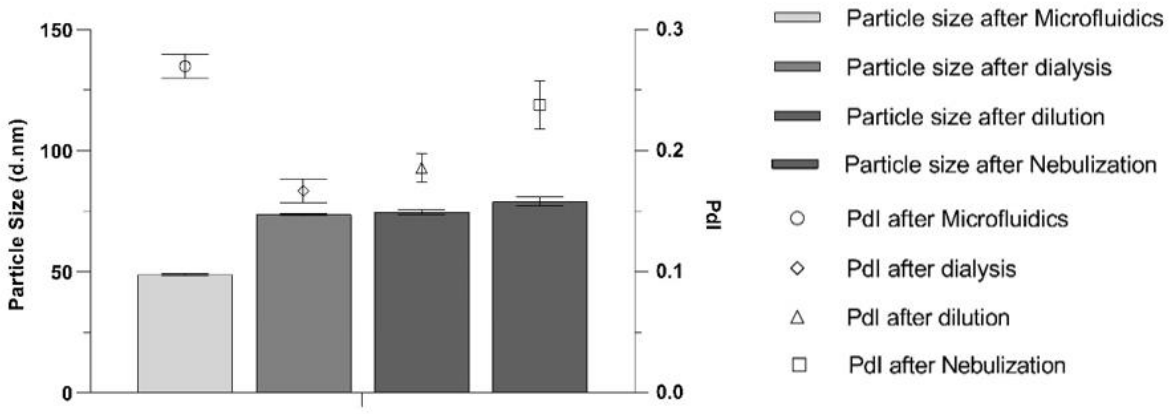

Graph 12 Particle size and PDI results of tRNA LNPs with PBS and E % T80 after microfluidics, after dialysis, after dilution, and after nebulization (n = 3).

Table 11 Encapsulation efficiencies of tRNA LNPs with PBS and E % T80 in a dilution ratio V/V 1:10 (n = 3)

Encapsulation Efficiency After Production (%)	**Encapsulation Efficiency After Dialysis (%)**	**Encapsulation Efficiency After Dilution (%)**	**Encapsulation Efficiency After Nebulization (%)**
99	99	98	94

In this formulation characterization, it was also evaluated osmolarity, pH (that for inhalation proposes should remain between 6.5 and 7.5, at 25 ºC), and particle surface charge through zeta potential measurements (that should be neutral) to increase the time the drug stays in the blood current and facilitate cellular uptake. The methods performed for characterizing the previous tests are described in subchapters 2.2.3 and 2.2.5. The results of all tests summarized in Table 12 complied with the quality attributes referred to before.

Table 12 pH, zeta potential, and osmolarity results throughout all process steps

	After Microfluidics	After dialysis	After Dilution	After Nebulization
pH (at 22 ºC)	---	---	7.4	---
Zeta potential (mV)	1.41	0.06	0.29	0.03
Osmolarity (mOsm)	---	781	320	317

pH value was only measured after dilution since there was not enough LNPs volume to perform pH measurements in all steps, so it was chosen to evaluate pH in the step where the solution would not have any additional formulation changes. The value obtained for pH at 22 ºC complied with quality attributes.

Zeta potential results showed that dialysis decreased surface charge, presenting neutral values, while osmolarity only achieved desirable values after dilution in PBS with E % T80 as reported before.

The results in Graph 13 show that the aerosol droplets formed in nebulization presented a normal deposition profile in the NGI stages when compared with that of the reference salbutamol solution. The average MMAD, GSD, and FPF values in Table 13 were also aligned with the reference solution, and, most importantly, the results complied with the target quality attributes of aerodynamic performance.

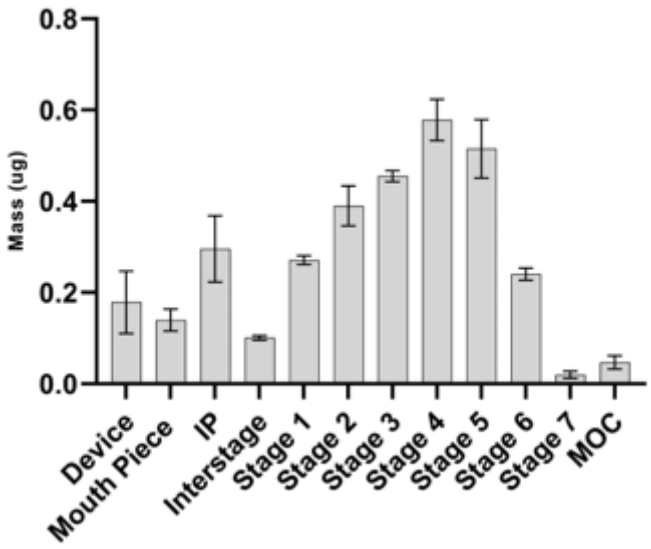

Graph 13 Mass deposition profile of formulation with PBS and E % T80 in the different stages (n = 2)

Table 13 Values of MMAD, GSD, and FPF for nebulization of formulation PBS with E % T80 (n = 2)

MMAD (µm)	GSD	FPF (%)
4.8	2.4	47

For aerodynamic performance evaluation, it was also performed a delivered dose test using the method described in subchapter 2.2.8, but there were found challenges in mass recovery. In this method, the recovery of the nebulized material is captured in a filter and then recovered by immersing and incubating the filter in a solvent. Even though the amount of solution nebulized was increased to augment detection, the concentration of tRNA in the solution is low and further dilutions decrease the effective concentration below the detection limit. Further improvement can be achieved by using more sensitive detection kits available commercially.

The polypropylene filter, described in the literature for delivered dose experiments, is hydrophobic and poses a challenge in the recovery of this aqueous solution, however, there is limited literature or guidelines regarding the type of filter or recovery strategies for nebulized RNA-LNPs. Even though it was not possible to reach optimum conditions for the accurate recovery of nebulized tRNA-LNPs, it is proposed to explore alternative hydrophilic filters (PTFE or cellulose) with comparable air resistance and use more sensitive detection kits.

The results of LNP particle characterization and the droplet's aerodynamic performance allowed to conclude that it was developed a robust nebulization platform for tRNA molecules encapsulated in LNPs that complies with all quality attributes for therapeutic use.

The initial proof of concept of LNPs and formulation optimization was performed using tRNA LNPs due to its affordability. Since mRNA is a very promising molecule used to develop new therapies, with more expression since Covid-19, the findings were extrapolated to prepare mRNA LNPs to perform nebulization.

3.7 Production and Characterization of nebulized mRNA-LNPs in PBS E % T80 (1:10) formulation

mRNA LNPs production was performed throughout the method described in subchapter 2.2.1 using a lipid phase composed of DC-Chol, DSPC, Cholesterol, and DMG-PEG 2000. In the aqueous phase, mRNA in a certain concentration was dissolved in sodium acetate aqueous solution. The only difference between the formulation used for mRNA and tRNA formulation was the modification of the lipid phase from cationic lipid DOTAP to ionizable lipid DC-Chol and in the aqueous phase from tRNA to mRNA. The lipid change was performed because, in previous works realized at Hovione, LNPs had a better performance when DC-Chol was used [73]. In the tRNA LNPs formulations, DC-Chol lipid was not used due to its higher cost in comparison with the DOTAP. The same characterization tests of subchapter 3.6 were performed to allow comparison between both formulations.

After microfluidics production, it was visible in

Graph 14 that mRNA LNPs had a higher particle size with 97.38 ± 1.20 nm with a PDI of 0.238 ± 0.010 than tRNA LNPs produced with the same conditions (particle size after microfluidics of 48.83 ± 0.52 and a PDI of 0.270 ± 0.010). The higher particle size was related to the larger size of the mRNA molecule in comparison with the tRNA molecule, approximately 1000 bp versus 70 bp, respectively. Other studies in the literature with mRNA LNPs with different compositions also reported particle sizes close to 100 nm for this type of system [135], [136].

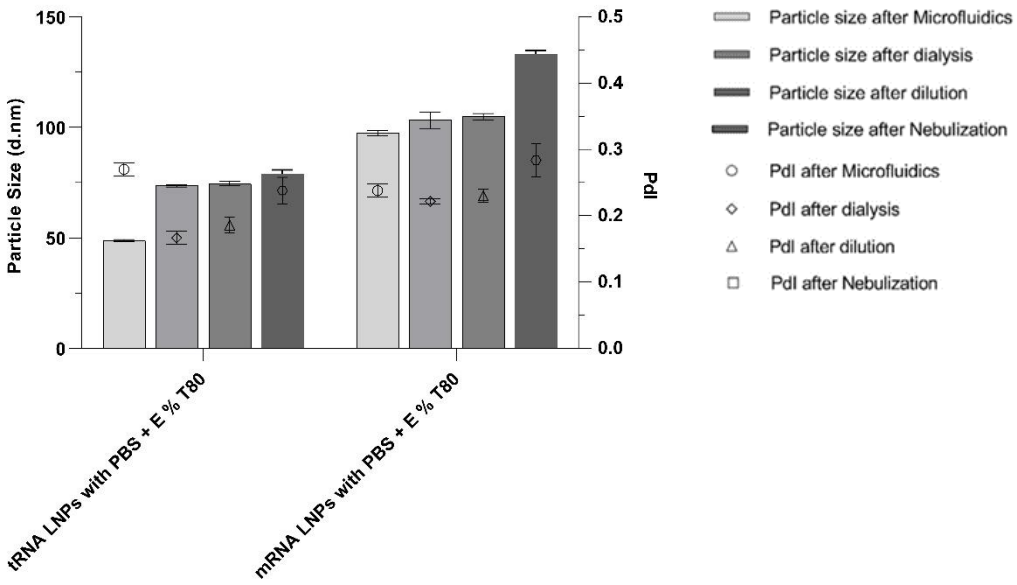

Graph 14 Particle size and PDI comparison between formulations that encapsulates tRNA and mRNA after production, after dialysis, after dilution, and after nebulization

Dialysis and dilution steps performed with the same buffer used in tRNA LNPs presented the same particle size, as shown in

Graph 14, although the size increase in mRNA LNPs was not so significant on the dialysis step as in the previous formulation.

When the mRNA LNPs were nebulized, there was a particle size increase from 104.4 ± 1.4 nm to 133.2 ± 1.7 nm and a PDI shift from 0.230 ± 0.010 to 0.284 ± 0.025. Since a single population was observed by DLS, aggregation/fusion of LNPs is unlikely. The mechanical stress might promote the relaxation of the nanoparticles and lead to swelling, but there is no published literature supporting this hypothesis. Despite this, the values were still inside defined quality attributes for this test (particle size < 200 nm and PDI < 0.300).

Osmolarity values presented in Table 14 for mRNA LNPs were higher than tRNA LNPs after dialysis, although the dilution performed resulted in LNPs with similar osmolarity to the previous formulation, which complies with quality attributes. The higher osmolality values detected in mRNA LNPs reflect a higher number of dissolved particles in the solution. The results from the encapsulation efficiency test are aligned with osmolality results, as there was a decrease in the EE of mRNA LNPs in comparison with tRNA LNPs after microfluidics production, as shown in Table 15.

This can indicate that not all mRNA molecules were encapsulated in the process, which may be explained by the size differences between tRNA and mRNA. Since the microfluidics parameters used were optimized for the tRNA molecule, when a larger molecule is used, the same parameters may not be suitable for an optimal mRNA encapsulation, so it will be necessary for future work to optimize some of the microfluidics parameters, like ionizable lipid concentration, N/P ratio, TFR, and FRR.

Table 14 Osmolarity comparison between mRNA LNPs and tRNA LNPs after dialysis, after dilution, and after nebulization

Sample	Osmolarity After dialysis (mOsm)	Osmolarity After dilution (mOsm)	Osmolarity After Nebulization (mOsm)
mRNA LNPs	1079	343	337
tRNA LNPs	781	320	317

Although the mRNA LNPs encapsulation efficiency in dialysis and nebulization decreased to 77 % and 72 % respectively, which was a value lower than the quality attribute established (EE > 80 %), these values are expected to increase after the optimization of the microfluidic process for this molecule.

Table 15 Encapsulation efficiency of mRNA LNPs with formulation PBS with E % T80, dilution ratio 1:10, after microfluidics, after dialysis, after dilution, and after nebulization

Sample	Encapsulation Efficiency After Production (%)	Encapsulation Efficiency After Dialysis (%)	Encapsulation Efficiency After Dilution (%)	Encapsulation Efficiency After Nebulization (%)
mRNA LNPs	85	77	76	72
tRNA LNPs	98	99	99	94

Despite this, the remaining characterization tests were executed to understand the mRNA integrity and aerodynamic performance after nebulization. Zeta potential and pH tests were not evaluated due to the lack of mRNA LNPs solution for the tests, although the formulation was not changed, thus it was expected that both parameters presented similar values to those reported for tRNA LNPs.

The mRNA integrity was assessed after microfluidics production, dialysis, dilution, and nebulization by IP-RP-HPLC. The chromatography method was developed to both quantify the amount of RNA but also to infer mRNA integrity (method described in subchapter 2.2.9). As an orthogonal method to infer mRNA integrity, agarose gel electrophoresis was performed for the same samples.

IP-RP-HPLC results (Table 16) did not show degradation of the mRNA during the production process, formulation, or nebulization since when comparing the unencapsulated mRNA sample (naked mRNA produced by the manufacturer) with the microfluidics sample, the percentage of impurities is similar.

Table 16 HPLC area of mRNA and impurity peaks of unencapsulated mRNA sample and microfluidic, diluted, and nebulization samples.

	mRNA peak		Impurities	
	Area (%)	STD	Area (%)	STD
Unencapsulated mRNA	79.4	0.9	20.6	0.9
Microfluidics	77.8	0.7	22.2	0.7
After Dilution	82.4	0.1	17.6	0.1
Nebulization (n =3)	77.7	8.8	22.3	8.8

The higher mRNA integrity percentage in dilution in comparison with the original microfluidic mRNA samples might be related to LNP lysis or mRNA ineffective extraction method. Nevertheless, the percentage of mRNA peak remains similar in all production steps which allows concluding that mRNA integrity remains stable during all process.

In the agarose gel electrophoresis (Figure 13), all samples were subjected to LNP lysis and mRNA extraction, except for the mRNA sample from the manufacturer. On lane number 5 (mRNA manufacturer's sample), it can be observed a single band migrated to the expected size (1000 bp), which indicates that the reference raw material sample has the expected quality as reported by the manufacturer. In the microfluidics sample (lane 7), it was possible to observe two fluorescent bands, one corresponding to the mRNA (1000 bp), and another heavier band (2000 bp). The latter might be a conjugation of the mRNA with the lipids that remain in the sample after LNPs lysis. Another possibility is that the process of LNPs lysis and mRNA extraction could lead to different mRNA conformations that would lead to the appearance of mRNA with a larger size and weight.

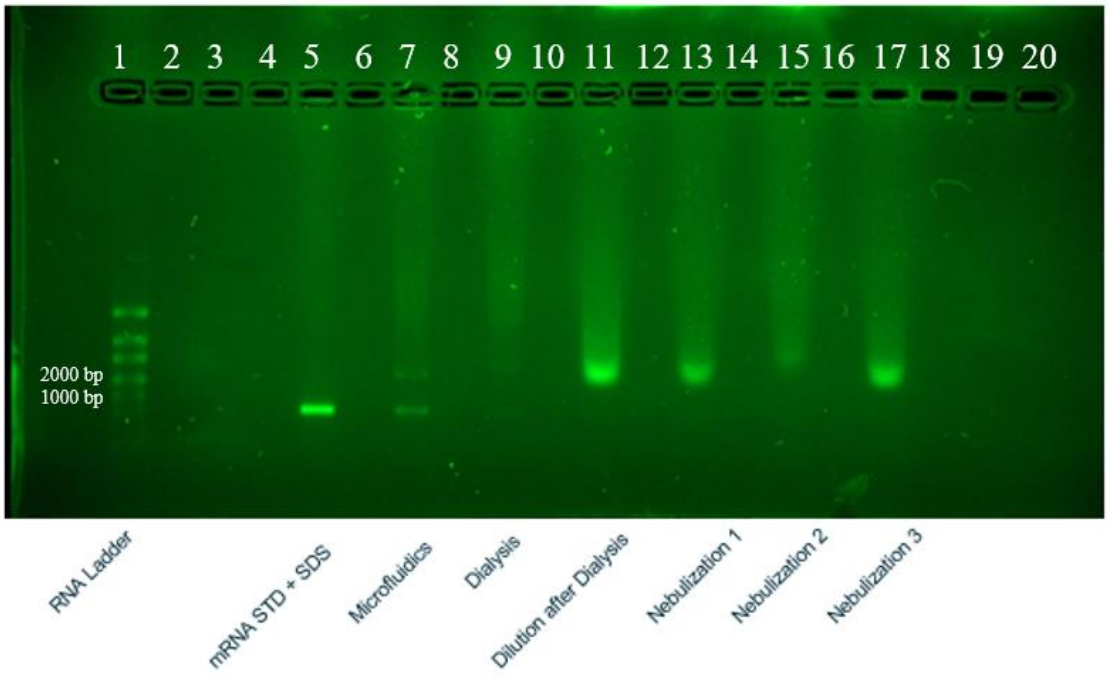

Figure 13 Gel electrophoresis comparison between RNA ladder and unencapsulated mRNA sample with SDS, microfluidic, dialysis, diluted dialysis, and three nebulization samples.

In the dialysis and nebulization samples (lanes 11, 13, 15, and 17), only the fluorescent band with 2000 bp appears. If it is assumed that this band corresponds to a different conformation of mRNA or mRNA conjugation with lipids, it is possible to conclude that after nebulization mRNA integrity remains, except in nebulization 2, where is noticeable a smear of the fluorescent band.

To evaluate if the heavier band is a conjugation of lipids with mRNA, future work should be done through an mRNA extraction process after LNPs lysis to separate mRNA and lipids, while evaluating the conformation theory, should be prepared a denaturing gel that will allow understanding of if the second band is a different conformation.

With mRNA formulation complying with the referred quality attributes, with the exception of EE, its aerodynamic performance was evaluated and compared with the tRNA formulation. Graph 15 reports a similar mass deposition profile, also aligned with the reference salbutamol solution. Table 17 shows that the results of MMAD, GSD, and FPF were very similar to the nebulized solution of tRNA LNPs, thus the formulation exhibits equivalent aerodynamic performance. Considering the small dimensions of the LNPs (< 100 nm), the variation in the size of LNPs containing tRNA or mRNA is not translated in different aerosol behavior, since droplets have a size 40 x larger than LNPs (in the range of 4 µm). These results comply with the quality attributes defined.

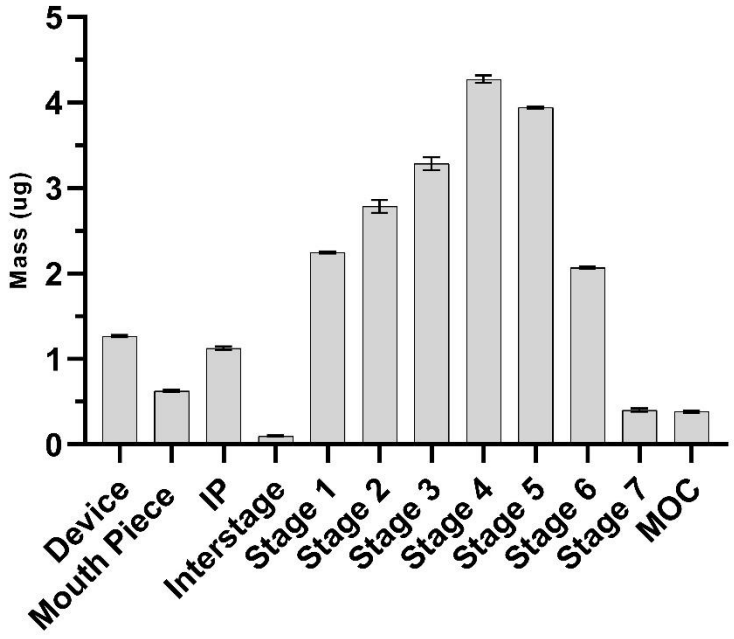

Graph 15 Mass distribution of mRNA LNPs formulation with PBS and E % T80 in the different stages of NGI

Table 17 Values of MMAD, GSD, and FPF for Nebulization of mRNA and tRNA LNPs formulation with PBS and E % T80

Sample	MMAD (µm)	GSD	FPF (%)
mRNA LNPs with PBS and E % T80	4.6	2.6	51
tRNA LNPs with PBS and E % T80	4.8	2.4	47

The delivered dose test using the method described in subchapter 2.2.8, was performed without success due to the challenges in mass recovery mentioned in the previous subchapter relative to tRNA formulations.

With these results, it was proven that a similar formulation used as a nebulization platform to tRNA can be used to deliver mRNA to the lungs, although some optimization is required to achieve optimal performance in all particle characterization and mRNA integrity tests.

4

CONCLUSIONS AND FUTURE PERSPECTIVES

In the present work, tRNA LNPs were produced through a microfluidics technique proven to be a replicable process, confirmed by the 19 batches produced with an average particle size of 48.88 ± 3.73 nm and a polydispersity index (PDI) of 0.198 ± 0.032, complying with the target quality attributes: particle size < 200nm, PDI < 0.300 and encapsulation efficiency (EE) > 80 %. Even though there is no available literature on encapsulated tRNA, the results observed were in accordance with the expected for lipid nanoparticles (LNPs) that encapsulate nucleic acid as payloads.

Stability studies showed that LNPs stored at 2-8 ºC and room temperature could maintain their particle size for up to 100 days. In this study, it was also concluded that LNPs should not be frozen at -20 ºC in any circumstances as it was observed an increase in size and PDI, possibly due to irreversible fusion or aggregation during the freezing process.

The produced batches were dialyzed in different excipient solutions to replace the solvent with a solvent system safe for inhalation and to protect the LNPs from the mechanical stress caused by the vibrating mesh nebulizer. PBS based solutions presented better results than NaCl 0.9 %, but none of the formulations initially tested maintained the LNPs colloidal stability after nebulization, since secondary populations were detected due to LNPs aggregation, fusion, or leakage. When osmolarity was optimized to physiological conditions (osmolarity between 300-310 mOsm), by performing a dilution ratio of 1:10 (V/V), it was concluded that the formulation in PBS with E % T80 was able to maintain the LNPs stability throughout the process, as the particle size and PDI were not significantly affected during dialysis and nebulization.

Therefore, a more extensive characterization was performed in the nebulized solution of PBS with E % T80 formulation, to show that it complied with the defined values for the critical quality attributes. This formulation was compatible with physiological conditions and ensured the stability of LNPs after nebulization with the following characteristics: particle size of 79 ± 1.87 nm with a PDI of 0.238 ± 0.02, an encapsulation value of 94 %, a neutral pH of 7.4 (at 22 ºC), a neutral zeta potential value of 0.03 mV and an osmolarity of 307 mOsm.

Moreover, evaluation of the aerodynamic performance showed that the aerosol droplets could reach the lungs with high efficiency, as the mass median aerodynamic diameter (MMAD) attained was 4.8 µm, being within the inhalable range (between 1 and 5 µm), with a geometric standard deviation (GSD) of 2.4 and a fine particle fraction (FPF) of 47 %. Even though the mass deposition profile showed a low mass recovery in lower stages, leading to higher MMAD values and lower FPF than the nebulizer's specification, the results for the formulations under study were very similar to the reference salbutamol solution, indicating that the formulation was appropriate for administration by nebulization. The nebulizer's mesh was likely impacted due to a defective cleaning process or nebulizer malfunction caused by excessive use, and future work should focus on optimizing the cleaning procedure to avoid impacting the nebulizer's mesh.

The formulation containing tRNA encapsulated in LNPs is the first product reported in the literature to present colloidal stability after nebulization and successfully comply with all key quality attributes defined, which opens the door for the future use of LNPs as an RNA vehicle for respiratory diseases. Thus, the same nebulization platform was used for mRNA, which is a molecule of high interest for new therapeutics and gained more expression since the commercialization of Covid-19 vaccines.

The microfluidics production process produced mRNA LNPs with a particle size two times higher than tRNA LNPs (97.38 ± 1.20 nm) and lower encapsulation efficiency (85 %). The larger particle size and lower encapsulation efficiency observed are related to the fact that the production process of LNPs was optimized for tRNA, a molecule that has a smaller size than mRNA (70 bp and 1000 bp respectively). Although these values have complied with the target key attributes, the production process of mRNA LNPs should be further optimized to increase the encapsulation efficiency by changing the N/P ratio, total flow rate, flow rate ratio, or ionizable lipid concentration. Nonetheless, mRNA LNPs were dialyzed and diluted in the previous best-performing formulation (PBS with E % T80). After nebulization, a particle size of 133.2 ± 1.7 nm, a PDI of 0.284 ± 0.025, and an encapsulation efficiency of 72 % were determined. While the particle size and PDI were within acceptable ranges, the low EE is expected to increase after the optimization of the microfluidic process for this molecule.

Since encapsulation efficiency is not critical to evaluate mRNA integrity inside LNPs nor the aerodynamic performance of the solution, these characterization tests were conducted. mRNA integrity was demonstrated throughout all process steps, from LNPs production until nebulization, since a single peak was detected by chromatography. However, in the agarose gel, the band size shifted from around 1000 bp to 2000 bp, which may indicate either a different mRNA conformation or conjugation with LNP material remaining from the extraction protocol. Future work should focus on the evaluation of the composition of the heavier band by preparing gel electrophoresis where mRNA samples are

extracted after LNPs lysis to separate mRNA from the lipids, and by running a denaturing gel to assess the possibility of a different mRNA conformation.

The good aerodynamic performance of the mRNA LNPs formulation in PBS with E % T80 was demonstrated by attaining the critical quality attributes within the acceptance range, with an MMAD of 4.6 µm, a GSD of 2.6, and an FPF of 51 %. These results were well aligned with the reference salbutamol solution and tRNA LNPs formulation, indicating the formulation developed has an aerodynamic performance capable of effectively delivering mRNA LNPs into the deep lungs.

It can be concluded that the work goals were attained, with the development of a proof of concept for a nebulization platform for the delivery of tRNA and mRNA into the lungs through inhalation, which are promising results for future RNA therapeutics for respiratory diseases. The present findings work as a proof of concept that good quality formulations of LNPs encapsulating RNA material can be developed for nebulization purposes. Most importantly, this work was a significant contribution to the field of nebulization of biopharmaceuticals, where the knowledge has been limited to the advancement of biotechnology but has been significantly boosted in the last years due to the pandemic.

5
BIBLIOGRAPHY

[1] "The top 10 causes of death." https://www.who.int/news-room/fact-sheets/detail/the-top-10-causes-of-death (accessed Jul. 11, 2022).

[2] S. Levine *et al.*, "The Global Impact of Respiratory Disease," 2021.

[3] "Respiratory Diseases Drugs Market Analysis, Size And Trends Global Forecast To 2022-2030." https://www.thebusinessresearchcompany.com/report/respiratory-disease-drugs-global-market-report (accessed Jul. 11, 2022).

[4] "The economic burden of lung disease." Accessed: Sep. 26, 2022. [Online]. Available: https://www.erswhitebook.org/chapters/the-economic-burden-of-lung-disease/

[5] L. Fala, "Nucala (Mepolizumab): First IL-5 Antagonist Monoclonal Antibody FDA Approved for Maintenance Treatment of Patients with Severe Asthma," *Am Health Drug Benefits*, vol. 9, 2016.

[6] W. Liang, H. W. Pan, D. Vllasaliu, and J. K. W. Lam, "Pulmonary delivery of biological drugs," *Pharmaceutics*, vol. 12, no. 11. MDPI AG, pp. 1–28, Nov. 01, 2020. doi: 10.3390/pharmaceutics12111025.

[7] Y. Lokko, M. Heijde, K. Schebesta, P. Scholtès, M. van Montagu, and M. Giacca, "Biotechnology and the bioeconomy—Towards inclusive and sustainable industrial development," *New Biotechnology*, vol. 40. Elsevier B.V., pp. 5–10, Jan. 25, 2018. doi: 10.1016/j.nbt.2017.06.005.

[8] "mRNA Vaccines & Therapeutics Market Growth Analysis Report." https://www.bccresearch.com/market-research/biotechnology/mrna-vaccines-and-therapeutics-market.html (accessed Jul. 11, 2022).

[9] "Francis Crick, Rosalind Franklin, James Watson, and Maurice Wilkins | Science History Institute." https://www.sciencehistory.org/historical-profile/james-watson-francis-crick-maurice-wilkins-and-rosalind-franklin (accessed Sep. 17, 2022).

[10] M. Cobb, "Who discovered messenger RNA?," *Current Biology*, vol. 25, no. 13. Cell Press, pp. R526–R532, Jun. 29, 2015. doi: 10.1016/j.cub.2015.05.032.

[11] Y.-K. Kim, "RNA Therapy: Current Status and Future Potential," *Chonnam Med J*, vol. 56, no. 2, p. 87, 2020, doi: 10.4068/cmj.2020.56.2.87.

[12] T. R. Damase, R. Sukhovershin, C. Boada, F. Taraballi, R. I. Pettigrew, and J. P. Cooke, "The Limitless Future of RNA Therapeutics," *Frontiers in Bioengineering and Biotechnology*, vol. 9. Frontiers Media S.A., Mar. 18, 2021. doi: 10.3389/fbioe.2021.628137.

[13] U. Sahin, K. Karikó, and Ö. Türeci, "MRNA-based therapeutics-developing a new class of drugs," *Nature Reviews Drug Discovery*, vol. 13, no. 10. Nature Publishing Group, pp. 759–780, Jan. 01, 2014. doi: 10.1038/nrd4278.

[14] X. Shen and D. R. Corey, "Chemistry, mechanism and clinical status of antisense oligonucleotides and duplex RNAs," *Nucleic Acids Res*, vol. 46, no. 4, pp. 1584–1600, Feb. 2018, doi: 10.1093/nar/gkx1239.

[15] M. L. Stephenson and P. C. Zamecnik, “Inhibition of Rous sarcoma viral RNA translation by a specific oligodeoxyribonucleotide (in vitro protein synthesis/nucleic acid hybridization/DNA nucleotidyltransferase),” 1978. [Online]. Available: https://www.pnas.org
[16] J. Wolff, R. Malone, P. Williams, and W. Chong, “Direct Gene transfer into mouse muscle in Vivo,” *Science (1979)*, vol. 247, pp. 1465–1468, 1990.
[17] J. A. Wolff *et al.*, “Direct Gene Transfer into Mouse Muscle in Vivo,” *Science (1979)*, vol. 247, no. 4949, pp. 1465–1468, 1990, doi: 10.1126/SCIENCE.1690918.
[18] X. Hou, T. Zaks, R. Langer, and Y. Dong, “Lipid nanoparticles for mRNA delivery,” *Nature Reviews Materials*, vol. 6, no. 12. Nature Research, pp. 1078–1094, Dec. 01, 2021. doi: 10.1038/s41578-021-00358-0.
[19] C. M. Perry and J. A. Barman Balfour, “Fomivirsen,” *Adis International Limited*, vol. 57, no. 3, pp. 375–380, 1999.
[20] D. Adams *et al.*, “Patisiran, an RNAi Therapeutic, for Hereditary Transthyretin Amyloidosis,” *New England Journal of Medicine*, vol. 379, no. 1, pp. 11–21, Jul. 2018, doi: 10.1056/NEJMOA1716153/SUPPL_FILE/NEJMOA1716153_DISCLOSURES.PDF.
[21] “Givlaari™ (givosiran) for the Treatment of Acute Hepatic Porphyria.” https://www.clinicaltrialsarena.com/projects/givlaari-givosiran/ (accessed Jul. 11, 2022).
[22] M. Y. T. Chow, Y. Qiu, and J. K. W. Lam, “Inhaled RNA Therapy: From Promise to Reality,” *Trends in Pharmacological Sciences*, vol. 41, no. 10. Elsevier Ltd, pp. 715–729, Oct. 01, 2020. doi: 10.1016/j.tips.2020.08.002.
[23] R. Feng, S. Patil, X. Zhao, Z. Miao, and A. Qian, “RNA Therapeutics - Research and Clinical Advancements,” *Frontiers in Molecular Biosciences*, vol. 8. Frontiers Media S.A., Sep. 22, 2021. doi: 10.3389/fmolb.2021.710738.
[24] “RNA interference (RNAi): by Nature Video - YouTube.” https://www.youtube.com/watch?v=cK-OGB1_ELE (accessed Jul. 28, 2022).
[25] “Transfer RNA (tRNA).” https://www.genome.gov/genetics-glossary/Transfer-RNA (accessed Aug. 31, 2022).
[26] “Overview of translation (article) | Khan Academy.” https://www.khanacademy.org/science/biology/gene-expression-central-dogma/translation-polypeptides/a/translation-overview (accessed Aug. 31, 2022).
[27] “tRNA therapies could help restore proteins lost in translation.” https://cen.acs.org/pharmaceuticals/drug-discovery/tRNA-therapies-help-restore-proteins/99/i34 (accessed Aug. 31, 2022).
[28] “Alltrna | The world’s first tRNA platform company.” https://www.alltrna.com/ (accessed Aug. 31, 2022).
[29] E. Dolgin, “tRNA therapeutics burst onto startup scene,” *Nat Biotechnol*, vol. 40, no. 3, pp. 283–286, Mar. 2022, doi: 10.1038/S41587-022-01252-Y.
[30] K.-J. Kim and A. B. Malik, “invited review Protein transport across the lung epithelial barrier,” 2003, doi: 10.1152/ajplung.00235.2002.-Alveolar.
[31] T. John, S. Vogel, R. Minshall, and K. Ridge, “Evidence for the role of alveolar epithelias gp60 in active transveolar albumin transport in the rat lung,” *Journal of physiology*, vol. 533, no. 2, pp. 547–559, 2001.
[32] J. Todoroff and R. Vanbever, “Fate of nanomedicines in the lungs,” *Current Opinion in Colloid and Interface Science*, vol. 16, no. 3. pp. 246–254, Jun. 2011. doi: 10.1016/j.cocis.2011.03.001.
[33] E. C. Mollocana-Lara, M. Ni, S. N. Agathos, and F. A. Gonzales-Zubiate, “The infinite possibilities of RNA therapeutics,” *J Ind Microbiol Biotechnol*, vol. 48, no. 9–10, 2021, doi: 10.1093/jimb/kuab063.
[34] K. Paunovska, D. Loughrey, and J. E. Dahlman, “Drug delivery systems for RNA therapeutics,” *Nature Reviews Genetics*, vol. 23, no. 5. Nature Research, pp. 265–280, May 01, 2022. doi: 10.1038/s41576-021-00439-4.

[35] J. S. Patton and P. R. Byron, “Inhaling medicines: Delivering drugs to the body through the lungs,” *Nature Reviews Drug Discovery*, vol. 6, no. 1. pp. 67–74, Jan. 2007. doi: 10.1038/nrd2153.
[36] L. Tan and X. Sun, “Recent advances in mRNA vaccine delivery,” *Nano Research*, vol. 11, no. 10. Tsinghua University Press, pp. 5338–5354, Oct. 01, 2018. doi: 10.1007/s12274-018-2091-z.
[37] H. Lv, S. Zhang, B. Wang, S. Cui, and J. Yan, “Toxicity of cationic lipids and cationic polymers in gene delivery,” *Journal of Controlled Release*, vol. 114, no. 1. pp. 100–109, Aug. 10, 2006. doi: 10.1016/j.jconrel.2006.04.014.
[38] L. A. Brito *et al.*, “A cationic nanoemulsion for the delivery of next-generation RNA vaccines,” *Molecular Therapy*, vol. 22, no. 12, pp. 2118–2129, Dec. 2014, doi: 10.1038/mt.2014.133.
[39] B. N. Aldosari, I. M. Alfagih, and A. S. Almurshedi, “Lipid nanoparticles as delivery systems for RNA-based vaccines,” *Pharmaceutics*, vol. 13, no. 2. MDPI AG, pp. 1–29, Feb. 01, 2021. doi: 10.3390/pharmaceutics13020206.
[40] C. B. Roces *et al.*, “Manufacturing considerations for the development of lipid nanoparticles using microfluidics,” *Pharmaceutics*, vol. 12, no. 11, pp. 1–19, Nov. 2020, doi: 10.3390/pharmaceutics12111095.
[41] X. Cheng and R. J. Lee, “The role of helper lipids in lipid nanoparticles (LNPs) designed for oligonucleotide delivery,” *Advanced Drug Delivery Reviews*, vol. 99. Elsevier B.V., pp. 129–137, Apr. 01, 2016. doi: 10.1016/j.addr.2016.01.022.
[42] X. Hou, T. Zaks, R. Langer, and Y. Dong, “Lipid nanoparticles for mRNA delivery,” *Nature Reviews Materials*, vol. 6, no. 12. Nature Research, pp. 1078–1094, Dec. 01, 2021. doi: 10.1038/s41578-021-00358-0.
[43] S. C. Semple, A. Chonn, and P. R. Cullis, “Influence of Cholesterol on the Association of Plasma Proteins with Liposomes †,” 1996.
[44] D. W. Sanders *et al.*, “Sars-cov-2 requires cholesterol for viral entry and pathological syncytia formation,” *Elife*, vol. 10, Apr. 2021, doi: 10.7554/ELIFE.65962.
[45] S. Patel *et al.*, “Naturally-occurring cholesterol analogues in lipid nanoparticles induce polymorphic shape and enhance intracellular delivery of mRNA,” *Nat Commun*, vol. 11, no. 1, Dec. 2020, doi: 10.1038/s41467-020-14527-2.
[46] D. Pozzi *et al.*, “Transfection efficiency boost of cholesterol-containing lipoplexes,” *Biochim Biophys Acta Biomembr*, vol. 1818, no. 9, pp. 2335–2343, Sep. 2012, doi: 10.1016/j.bbamem.2012.05.017.
[47] J. v. Jokerst, T. Lobovkina, R. N. Zare, and S. S. Gambhir, “Nanoparticle PEGylation for imaging and therapy,” *Nanomedicine*, vol. 6, no. 4. pp. 715–728, Jun. 2011. doi: 10.2217/nnm.11.19.
[48] E. Samaridou, J. Heyes, and P. Lutwyche, “Lipid nanoparticles for nucleic acid delivery: Current perspectives,” *Advanced Drug Delivery Reviews*, vol. 154–155. Elsevier B.V., pp. 37–63, Jan. 01, 2020. doi: 10.1016/j.addr.2020.06.002.
[49] R. C. Ryals, S. Patel, C. Acosta, M. McKinney, M. E. Pennesi, and G. Sahay, “The effects of PEGylation on LNP based mRNA delivery to the eye,” *PLoS One*, vol. 15, no. 10 October, Oct. 2020, doi: 10.1371/journal.pone.0241006.
[50] M. S. Webb Ayb *et al.*, “Comparison of di¡erent hydrophobic anchors conjugated to poly(ethylene glycol): e¡ects on the pharmacokinetics of liposomal vincristine,” 1998.
[51] “Definition of Pharmaceutical Excipients - pharma excipients.” https://www.pharmaexcipients.com/pharmaceutical-excipients-some-definition/ (accessed Sep. 14, 2022).
[52] P. Baldrick, “Pharmaceutical excipient development: The need for preclinical guidance,” *Regulatory Toxicology and Pharmacology*, vol. 32, no. 2, pp. 210–218, 2000, doi: 10.1006/rtph.2000.1421.

[53] L. Schoenmaker *et al.*, "mRNA-lipid nanoparticle COVID-19 vaccines: Structure and stability," *International Journal of Pharmaceutics*, vol. 601. Elsevier B.V., May 15, 2021. doi: 10.1016/j.ijpharm.2021.120586.
[54] G. Pilcer and K. Amighi, "Formulation strategy and use of excipients in pulmonary drug delivery," *International Journal of Pharmaceutics*, vol. 392, no. 1–2. pp. 1–19, Jun. 2010. doi: 10.1016/j.ijpharm.2010.03.017.
[55] D. L. Johnson, T. A. Pearce, and N. A. Esmen, "The effect of phosphate buffer on aerosol size distribution of nebulized Bacillus subtilis and Pseudomonas fluorescens bacteria," *Aerosol Science and Technology*, vol. 30, no. 2, pp. 202–210, 1999, doi: 10.1080/027868299304787.
[56] R. Respaud *et al.*, "Effect of formulation on the stability and aerosol performance of a nebulized antibody," *MAbs*, vol. 6, no. 5, pp. 1347–1355, Sep. 2014, doi: 10.4161/mabs.29938.
[57] W. Wang, S. Singh, D. L. Zeng, K. King, and S. Nema, "Antibody structure, instability, and formulation," *Journal of Pharmaceutical Sciences*, vol. 96, no. 1. John Wiley and Sons Inc., pp. 1–26, 2007. doi: 10.1002/jps.20727.
[58] T. Anchordoquy, D. Allison, M. Molina, L. Girouard, and T. Carson, "Physical stabilization of DNA-Based therapeutics," *Research focus*, vol. 6, pp. 463–470, 2001.
[59] W. Abdelwahed, G. Degobert, S. Stainmesse, and H. Fessi, "Freeze-drying of nanoparticles: Formulation, process and storage considerations," *Advanced Drug Delivery Reviews*, vol. 58, no. 15. Elsevier, pp. 1688–1713, Dec. 30, 2006. doi: 10.1016/j.addr.2006.09.017.
[60] B. K. Muralidhara, R. Baid, S. M. Bishop, M. Huang, W. Wang, and S. Nema, "Critical considerations for developing nucleic acid macromolecule based drug products," *Drug Discovery Today*, vol. 21, no. 3. Elsevier Ltd, pp. 430–444, Mar. 01, 2016. doi: 10.1016/j.drudis.2015.11.012.
[61] J. A. Kulkarni, D. Witzigmann, S. Chen, P. R. Cullis, and R. van der Meel, "Lipid Nanoparticle Technology for Clinical Translation of siRNA Therapeutics," *Acc Chem Res*, vol. 52, no. 9, pp. 2435–2444, Sep. 2019, doi: 10.1021/acs.accounts.9b00368.
[62] I. Maclachlan, "Liposomal Formulations for Nucleic Acid Delivery," 2007.
[63] S. J. Shepherd, D. Issadore, and M. J. Mitchell, "Microfluidic formulation of nanoparticles for biomedical applications," *Biomaterials*, vol. 274. Elsevier Ltd, Jul. 01, 2021. doi: 10.1016/j.biomaterials.2021.120826.
[64] A. Wagner, K. Vorauer-Uhl, G. Kreismayr, and H. Katinger, "The crossflow injection technique: An improvement of the ethanol injection method," *J Liposome Res*, vol. 12, no. 3, pp. 259–270, 2002, doi: 10.1081/LPR-120014761.
[65] B. G. Carvalho, B. T. Ceccato, M. Michelon, S. W. Han, and L. G. de la Torre, "Advanced Microfluidic Technologies for Lipid Nano-Microsystems from Synthesis to Biological Application," *Pharmaceutics*, vol. 14, no. 1, p. 141, Jan. 2022, doi: 10.3390/pharmaceutics14010141.
[66] S. Batzri and Korn Edward, "Single bilayer Lipossomes prepared without sonication," *Biochim Biophys Acta*, vol. 298, pp. 1015–1019, 1973.
[67] M. J. W. Evers, J. A. Kulkarni, R. van der Meel, P. R. Cullis, P. Vader, and R. M. Schiffelers, "State-of-the-Art Design and Rapid-Mixing Production Techniques of Lipid Nanoparticles for Nucleic Acid Delivery," *Small Methods*, vol. 2, no. 9. John Wiley and Sons Inc, Sep. 11, 2018. doi: 10.1002/SMTD.201700375.
[68] D. Liu, H. Zhang, F. Fontana, J. T. Hirvonen, and H. A. Santos, "Current developments and applications of microfluidic technology toward clinical translation of nanomedicines."
[69] M. A. Tomeh and X. Zhao, "Recent Advances in Microfluidics for the Preparation of Drug and Gene Delivery Systems," *Molecular Pharmaceutics*, vol. 17, no. 12. American Chemical Society, pp. 4421–4434, Dec. 07, 2020. doi: 10.1021/acs.molpharmaceut.0c00913.
[70] E. A. Mansur, Y. Mingxing, W. Yundong, and D. Youyuan, "A State-of-the-Art Review of Mixing in Microfluidic Mixers *," 2008.
[71] M. S. Williams, K. J. Longmuir, and P. Yager, "A practical guide to the staggered herringbone mixer," *Lab Chip*, vol. 8, no. 7, pp. 1121–1129, 2008, doi: 10.1039/b802562b.

[72] C. Webb *et al.*, "Using microfluidics for scalable manufacturing of nanomedicines from bench to GMP: A case study using protein-loaded liposomes," *Int J Pharm*, vol. 582, May 2020, doi: 10.1016/j.ijpharm.2020.119266.
[73] Lopes Carolina, "Development and Characterization of RNA-loaded Lipid Nanoparticles prepared by Microfluidics Technique," Instituto suoerior técnico, Lisboa, 2021.
[74] H. Zhang, J. Leal, M. R. Soto, H. D. C. Smyth, and D. Ghosh, "Aerosolizable lipid nanoparticles for pulmonary delivery of mRNA through design of experiments," *Pharmaceutics*, vol. 12, no. 11, pp. 1–16, Nov. 2020, doi: 10.3390/pharmaceutics12111042.
[75] N. M. Belliveau *et al.*, "Microfluidic synthesis of highly potent limit-size lipid nanoparticles for in vivo delivery of siRNA," *Mol Ther Nucleic Acids*, vol. 1, no. 8, p. e37, 2012, doi: 10.1038/mtna.2012.28.
[76] M. Maeki *et al.*, "Understanding the formation mechanism of lipid nanoparticles in microfluidic devices with chaotic micromixers," *PLoS One*, vol. 12, no. 11, Nov. 2017, doi: 10.1371/journal.pone.0187962.
[77] "Routes of Drug Administration." https://www.medindia.net/patientinfo/routes-of-drug-administration.htm (accessed Sep. 18, 2022).
[78] "Routes of Drug Administration | KnowledgeDose." https://www.knowledgedose.com/routes-of-drug-administration/ (accessed Sep. 18, 2022).
[79] J. Grossman, "The Evolution of Inhaler Technology," 1994.
[80] C. J. Miller, "Inhaled medications," in *Small Animal Critical Care Medicine, Second Edition*, Elsevier Health Sciences, 2014, pp. 903–906. doi: 10.1016/B978-1-4557-0306-7.00172-0.
[81] M. Ibrahim, R. Verma, and L. Garcia-Contreras, "Inhalation drug delivery devices: Technology update," *Medical Devices: Evidence and Research*, vol. 8. Dove Medical Press Ltd, pp. 131–139, Feb. 12, 2015. doi: 10.2147/MDER.S48888.
[82] "Advantages and disadvantages for inhalers | RESPe." http://www.respelearning.scot/topic-3-treatment/inhalers/advantages-and-disadvantages-inhalers (accessed Jul. 28, 2022).
[83] M. Newhouse, "Advantages of Pressurized Canister Metered Dose Inhalers," Mary Ann Liebert, Inc., Pubiishers, 1991.
[84] S. P. Sahane, A. K. Nikhar, S. Bhaskaran, and D. R. Mundhada, "Dry Powder Inhaler: An Advance Technique for Pulmonary Drug Delivery System," *INTERNATIONAL JOURNAL OF PHARMACEUTICAL AND CHEMICAL SCIENCES* , vol. 1, no. 3, pp. 1375–1383, 2012, [Online]. Available: www.ijpcsonline.com1376
[85] I. Khan, S. Yousaf, M. A. Alhnan, W. Ahmed, A. Elhissi, and M. J. Jackson, "Design characteristics of inhaler devices used for pulmonary delivery of medical aerosols," in *Surgical Tools and Medical Devices, Second Edition*, Springer International Publishing, 2016, pp. 573–592. doi: 10.1007/978-3-319-33489-9_19.
[86] S. D. McCarthy, H. E. González, and B. D. Higgins, "Future trends in nebulized therapies for pulmonary disease," *Journal of Personalized Medicine*, vol. 10, no. 2. MDPI AG, May 01, 2020. doi: 10.3390/jpm10020037.
[87] J. Lourenço, "Administração de Fármacos por Via Inalatória-Uma Via Promissora," 2014.
[88] O. N. M. Mccallion, K. M. G. Taylor A', P. A. Bridges%, M. Thomas, and A. J. Taylor, "international journal of pharmaceutics Invited Review Jet nebulisers for pulmonary drug delivery," 1996.
[89] S. W. Stein and C. G. Thiel, "The History of Therapeutic Aerosols: A Chronological Review," *Journal of Aerosol Medicine and Pulmonary Drug Delivery*, vol. 30, no. 1. Mary Ann Liebert Inc., pp. 20–41, Feb. 01, 2017. doi: 10.1089/jamp.2016.1297.
[90] P. Bajpai, "Hydraulics," in *Biermann's Handbook of Pulp and Paper*, Elsevier, 2018, pp. 455–482. doi: 10.1016/B978-0-12-814238-7.00023-4.
[91] T. C. Carvalho and J. T. McConville, "The function and performance of aqueous aerosol devices for inhalation therapy," *Journal of Pharmacy and Pharmacology*, vol. 68, no. 5. Blackwell Publishing Ltd, pp. 556–578, May 01, 2016. doi: 10.1111/jphp.12541.

[92] J. Dhanani, J. F. Fraser, H. K. Chan, J. Rello, J. Cohen, and J. A. Roberts, “Fundamentals of aerosol therapy in critical care,” *Critical Care*, vol. 20, no. 1. BioMed Central Ltd., Oct. 07, 2016. doi: 10.1186/s13054-016-1448-5.
[93] J. N. Pritchard, R. H. M. Hatley, J. Denyer, and Di. von Hollen, “Mesh nebulizers have become the first choice for new nebulized pharmaceutical drug developments,” *Ther Deliv*, vol. 9, no. 2, pp. 121–136, Feb. 2018, doi: 10.4155/tde-2017-0102.
[94] L. Y. Yeo, J. R. Friend, M. P. McIntosh, E. N. Meeusen, and D. A. Morton, “Ultrasonic nebulization platforms for pulmonary drug delivery,” *Expert Opinion on Drug Delivery*, vol. 7, no. 6. pp. 663–679, Jun. 2010. doi: 10.1517/17425247.2010.485608.
[95] C. O’Callaghan and P. Barry, “The science of nebulised drug delivery,” *Thorax*, vol. 52, no. Supplement 2, pp. 31–31, Apr. 1997, doi: 10.1136/thx.52.suppl_2.31.
[96] J. S. Lass, A. Sant, and M. Knoch, “New advances in aerosolised drug delivery: Vibrating membrane nebuliser technology,” *Expert Opin Drug Deliv*, vol. 3, no. 5, pp. 693–702, Sep. 2006, doi: 10.1517/17425247.3.5.693.
[97] C. O’Callaghan and P. Barry, “The science of nebulised drug delivery,” *Thorax*, vol. 52, no. Supplement 2, pp. 31–31, Apr. 1997, doi: 10.1136/thx.52.suppl_2.31.
[98] S. Newman, “Aerosols,” *Aerosols*, pp. 58–64, 2006.
[99] C. Evans and L. Mao, “QUALITY BY DESIGN IN INHALATION PRODUCT DEVELOPMENT,” 2014. [Online]. Available: www.ondrugdelivery.com
[100] J. Gaspar, “Analytial quality by desigh to charchterize inhalation products,” 2018.
[101] M. Longmire, P. L. Choyke, and H. Kobayashi, “Clearance properties of nano-sized particles and molecules as imaging agents: Considerations and caveats,” *Nanomedicine*, vol. 3, no. 5. pp. 703–717, Oct. 2008. doi: 10.2217/17435889.3.5.703.
[102] E. Blanco, H. Shen, and M. Ferrari, “Principles of nanoparticle design for overcoming biological barriers to drug delivery,” *Nature Biotechnology*, vol. 33, no. 9. Nature Publishing Group, pp. 941–951, Sep. 08, 2015. doi: 10.1038/nbt.3330.
[103] M. Instruments, “Zetasizer Nano User Manual MAN0485 Issue 1.1 April 2013 English,” 2007.
[104] A. Sukhanova, S. Bozrova, P. Sokolov, M. Berestovoy, A. Karaulov, and I. Nabiev, “Dependence of Nanoparticle Toxicity on Their Physical and Chemical Properties,” *Nanoscale Research Letters*, vol. 13. Springer New York LLC, 2018. doi: 10.1186/s11671-018-2457-x.
[105] A. Barhoum, M. L. García-Betancourt, H. Rahier, and G. van Assche, “Physicochemical characterization of nanomaterials: Polymorph, composition, wettability, and thermal stability,” in *Emerging Applications of Nanoparticles and Architectural Nanostructures: Current Prospects and Future Trends*, Elsevier Inc., 2018, pp. 255–278. doi: 10.1016/B978-0-323-51254-1.00009-9.
[106] “IACUC Policies, procedures and guidelines,” 2010. [Online]. Available: https://olaw.nih.gov/guidance/faqs#F
[107] “OSMOLALITY AND OSMOLARITY,” 2020, doi: 10.31003/USPNF_M99580_03_01.
[108] “Osmolarity and Osmolality – Advanced Renal Education Program.” https://advancedrenaleducation.com/wparep/article/osmolarity-and-osmolality/ (accessed Aug. 02, 2022).
[109] “Freezing Point Osmometer Instructions K-7400S Semi-Micro Osmometer,” 2022. [Online]. Available: www.knauer.net
[110] K. N. Desager, H. P. van Bever, and W. J. Stevens, “Osmolality and pH of anti-asthmatic drug solutions,” 1990.
[111] “pH and Water | U.S. Geological Survey.” https://www.usgs.gov/special-topics/water-science-school/science/ph-and-water (accessed Aug. 02, 2022).
[112] J. Z. Porterfield and A. Zlotnick, “A simple and general method for determining the protein and nucleic acid content of viruses by UV absorbance,” *Virology*, vol. 407, no. 2, pp. 281–288, Nov. 2010, doi: 10.1016/j.virol.2010.08.015.
[113] L. J. Jones, S. T. Yue, C.-Y. Cheung, and V. L. Singer, “RNA Quantitation by Fluorescence-Based Solution Assay: RiboGreen Reagent Characterization,” 1998.

[114] J. Currie, J. R. Dahlberg, J. Eriksson, F. Schweikart, G. A. Nilsson, and E. Örnskov, "Stability Indicating Ion-Pair Reversed-Phase Liquid Chromatography Method for Modified mRNA."
[115] I. C. Santos and J. S. Brodbelt, "Recent developments in the characterization of nucleic acids by liquid chromatography, capillary electrophoresis, ion mobility, and mass spectrometry (2010–2020)," *Journal of Separation Science*, vol. 44, no. 1. Wiley-VCH Verlag, pp. 340–372, Jan. 01, 2021. doi: 10.1002/jssc.202000833.
[116] E. Paredes, V. Aduda, K. L. Ackley, and H. Cramer, "Manufacturing of Oligonucleotides," in *Comprehensive Medicinal Chemistry III*, Elsevier, 2017, pp. 233–279. doi: 10.1016/b978-0-12-409547-2.12423-0.
[117] "Physical Tests and Determinations," 2012.
[118] S. Nayak, P. Ghugare, and B. Vaidhun, "EVALUATION OF AERODYNAMIC PARTICLE SIZE DISTRIBUTION OF DRUGS USED IN INHALATION THERAPY: A CONCISE REVIEW," *International Journal of Research -GRANTHAALAYAH*, vol. 8, no. 7, pp. 264–271, Aug. 2020, doi: 10.29121/GRANTHAALAYAH.V8.I7.2020.579.
[119] "Driving Results In Inhaler Testing 2021." https://pt.calameo.com/copleyscientific/read/006693220fa76cad62867?page=122 (accessed Jul. 29, 2022).
[120] N. Nimmano and S. B. Mohd Mohari, "Comparison of efficacies of full and abbreviated cascade impactors in aerosol characterization of nebulized salbutamol sulfate produced by a jet nebulizer," *Pharmacia*, vol. 68, no. 4, pp. 899–905, 2021, doi: 10.3897/pharmacia.68.e76072.
[121] "Anaesthetic and respiratory equipment-Nebulizing systems and components," 2013.
[122] H. Douafer, V. Andrieu, J. Michel Brunel, and J.-M. Brunel, "Scope and limitations on aerosol drug delivery for the treatment of infectious respiratory diseases", doi: 10.1016/j.jconrel.2020.07.002ï.
[123] "Driving Results In Inhaler Testing 2021." https://pt.calameo.com/copleyscientific/read/006693220fa76cad62867?page=48 (accessed Sep. 20, 2022).
[124] L. J. Jones, S. T. Yue, C.-Y. Cheung, and V. L. Singer, "RNA Quantitation by Fluorescence-Based Solution Assay: RiboGreen Reagent Characterization," 1998.
[125] "FAQ | Dolomite Microfluidics." https://www.dolomite-microfluidics.com/support/faq/ (accessed Sep. 20, 2022).
[126] R. van der Meel *et al.*, "Modular Lipid Nanoparticle Platform Technology for siRNA and Lipophilic Prodrug Delivery," *Small*, vol. 17, no. 37, Sep. 2021, doi: 10.1002/smll.202103025.
[127] CHMP, "Committee for Medicinal Products for Human Use (CHMP) Assessment report," 2018. [Online]. Available: www.ema.europa.eu/contact
[128] Y. Suzuki, K. Hyodo, Y. Tanaka, and H. Ishihara, "SiRNA-lipid nanoparticles with long-term storage stability facilitate potent gene-silencing in vivo," *Journal of Controlled Release*, vol. 220, pp. 44–50, Dec. 2015, doi: 10.1016/j.jconrel.2015.10.024.
[129] R. Lball, P. Bajaj, and K. A. Whitehead, "Achieving long-term stability of lipid nanoparticles: Examining the effect of pH, temperature, and lyophilization," *Int J Nanomedicine*, vol. 12, pp. 305–315, 2017, doi: 10.2147/IJN.S123062.
[130] J. C. Kasper and W. Friess, "The freezing step in lyophilization: Physico-chemical fundamentals, freezing methods and consequences on process performance and quality attributes of biopharmaceuticals," *European Journal of Pharmaceutics and Biopharmaceutics*, vol. 78, no. 2. pp. 248–263, Jun. 2011. doi: 10.1016/j.ejpb.2011.03.010.
[131] W. Abdelwahed, G. Degobert, S. Stainmesse, and H. Fessi, "Freeze-drying of nanoparticles: Formulation, process and storage considerations," *Advanced Drug Delivery Reviews*, vol. 58, no. 15. Elsevier, pp. 1688–1713, Dec. 30, 2006. doi: 10.1016/j.addr.2006.09.017.
[132] P. v. Date, A. Samad, and P. v. Devarajan, "Freeze thaw: A simple approach for prediction of optimal cryoprotectant for freeze drying," *AAPS PharmSciTech*, vol. 11, no. 1, pp. 304–313, Mar. 2010, doi: 10.1208/s12249-010-9382-3.

[133] T. Terada *et al.*, “Characterization of Lipid Nanoparticles Containing Ionizable Cationic Lipids Using Design-of-Experiments Approach,” *Langmuir*, vol. 37, no. 3, pp. 1120–1128, Jan. 2021, doi: 10.1021/acs.langmuir.0c03039.
[134] Philips, *Philips Innospire go - instructions manual*. [Online]. Available: www.Manualslib.com
[135] J. Kim *et al.*, “Engineering Lipid Nanoparticles for Enhanced Intracellular Delivery of mRNA through Inhalation,” *ACS Nano*, Aug. 2022, doi: 10.1021/acsnano.2c05647.
[136] H. Zhang, J. Leal, M. R. Soto, H. D. C. Smyth, and D. Ghosh, “Aerosolizable lipid nanoparticles for pulmonary delivery of mRNA through design of experiments,” *Pharmaceutics*, vol. 12, no. 11, pp. 1–16, Nov. 2020, doi: 10.3390/pharmaceutics12111042.